Ontario

We are committed to providing accessible customer service.
If you need accessible formats or communications supports, please contact us.

Nous tenons à améliorer l'accessibilité des services à la clientèle.
Si vous avez besoin de formats accessibles ou d'aide à la communication, veuillez nous contacter.

COMPLEX STRUCTURAL STUDY
OF THE HUFFMAN TWP. PROPERTY
HUFFMAN TOWNSHIP
NTS Sheet 1: 50, 000
041O09

For
RICHMOND MINERALS INC

Author:
Vadim Galkine, P.Geo, Ph D, Dr of Sci.
January 12**, 2022**

Contents

Summary

Complex Structural Study of the Huffman Twp. Property (Richmond Minerals Inc) was completed using several different independent datasets. They included optical datasets (satellite images of different resolution and band combinations, aerial photo), topography, and DEM data.

The data were processed into the tables with all the lineaments and their various intersections counts, and additional weighting procedure was applied to the data. All the partial datasets were converted into grids and represented as contour density maximums maps in Surfer and ArcMap.

Obtained contour maps of lineament densities repeatedly show areas with high lineament (and their various intersections) densities in several spatially stable locations. These zones are considered as the most favorable for mineralization from the method foundations standpoint, and may be recommended as the first-order target zones for future exploration activities. Although the Exploration Target Maps represent the most reliable targets, the individual Density Maps of lineaments and their intersections may be used for the exploration planning as well.

Rose-diagrams for Secondary lineaments orientation have been constructed. Interpretation of the main lineament trends leads to the assumption that area of the perpendicular orientation trends “collision” may be favorable for fluid flow during the deformation, and consequently, for mineralization.

Analogue modeling (plastic/rupture and elastic fields) results show that there exist some spatially stable zones with the highest deformation and fracturing (plastic) or the lowest stress (elastic) in various geodynamic stress fields. These zones – from the modeling standpoint – may be taken as the most favorable for the future exploration activities. The Exploration Target Maps based on the Modeling have been built.

By combining the results obtained by Structural Lineament Analysis and Physical Modeling we built Primary Target Map. From the Complex Structural Analysis standpoint, these targets should be taken as the areas for the future exploration activities.

It is also important to use the partial (not final) target maps obtained by separate processing stages of Remote Exploration Method.

Further improvements of the target maps can result from the updating the existing maps with field structural observations, geochemical and/or geophysical surveys.

Introduction

At the request of Mr. Warren Hawkins, P. Eng., Exploration Manager, this report has been prepared by Dr. Vadim Galkine (Ph.D., Dr.Sci, P.Geo), 2325098 Ontario Inc, to present the results of the Remote Exploration Technique (Structural Lineament Analysis) application on Richmond Minerals Inc Huffman Twp. Property , ON, Canada.

All coordinates in this report correspond to the NAD83 UTM_Zone_17N.

No geological/geophysical/geochemical data have been analyzed apart of the short prospector report written by J. SALO (June 12, 2017). The report covers two mining claims held in Huffman Township, Porcupine Mining Division; 4283172 and 4283173 both being single units.

Remote Exploration Technique.

The reader can learn more details on the method at the www.remoteexploration.com web page

Method of ***Remote Exploration*** (Figure 1) used here includes the following **consequent techniques**:

Part I.

- **Structural Lineament (fault and fractures) Analysis** using DEM and satellite data of various sources available for purchase or free of charge through Internet. The main analysis itself is purely *manual* procedure. Hence, apart from natural occasional human errors, and distortions or the flaws of the images, no artificial systemic errors (such as automatic processing bias) affect the results. In recent years new methods of *automatic deciphering* of lineaments are being developed. Two of such new methods are adopted by author as an addition to manual analysis.

- **Processing of the data** with various computer programs (custom-built and commercial) and creating contour maps of lineament densities and strain levels for the area
- **Analyzing the data spatially** and outlining the areas which should be the Primary Exploration Targets from the standpoint of the method.
- **Physical (analogue)** modeling of the main lineament/structural frame mechanical response to the different geodynamic conditions
- **Processing of the data** with various computer programs (custom-built and commercial) and creating contour maps of lineament densities and strain levels for the area
- **Analyzing the data spatially** and outlining the areas which should be the Primary Exploration Targets from the standpoint of the method.

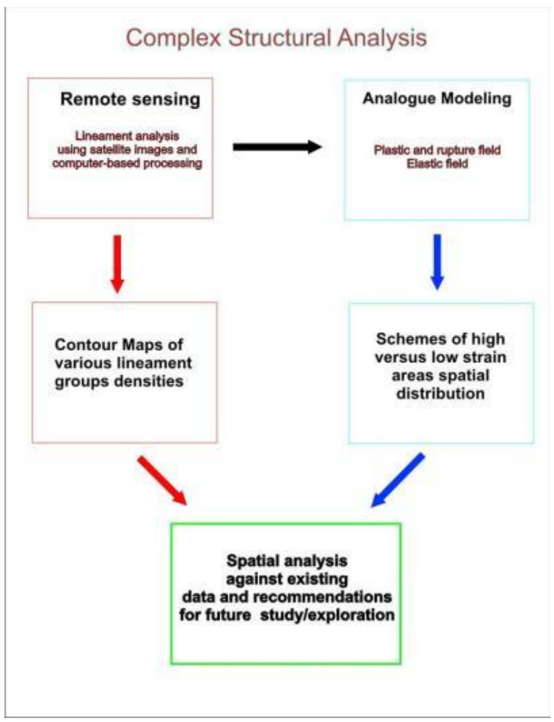

Figure 1. Main stages of the method applied to the area.

Structural Lineament Analysis foundations

Lineaments can be defined as linear surface features, visible on a map. Accordingly, one may speak of topographic, photo-, satellite, geological, geophysical lineaments etc. In our study we deal with photo- and topographic lineaments. These linear features, as a matter of fact, represent the surface reflection (projection) of either a geological body (such as a dyke or a layer, bed, intrusion) or of a plane of anomalous physical property - such as fault rupture, zone of mechanical weakness (or hardness), zone of high (low) permeability etc. Hence, by studying lineaments, we indirectly study the surface pattern of the physical properties, mainly – the distribution of fractures and faults projection on the earth's surface.

Lineament analysis as a method of obtaining new geological information has been in existence for at least 50 years. "Pros" and "contras" of the method have been discussed in numerous papers. The method is considered to be a "mainstream" in hydrogeology, where the direct links between water accumulation and fractures density pattern has been proved. Direct link with mineralization is not that straightforward, since the mineralization is often geologically old, and the lineaments observed are believed to be of somewhat recent age. On the other hand, more and more data are being published that prove the fact that the visible lineaments inherit to rather larger extent the pattern of pre-existing fractures.

In 1980-s a lot of papers were published with the results showing that statistically relevant correlation exists between regional (or even global) network of lineaments and spatial distribution of the mineral deposits [1]. Even relatively recently Carlos J.Chernicoff et al. [2] argued that there exists an un-doubtful crustal lineament control on magmatism and mineralization in north-western Argentina. We will leave the discussion outside the scope of the current study. Let us note, nevertheless, that while there might be a disagreement amongst the geologists with regard to spatial correlation of mineral deposits versus lineaments of unknown nature, everybody agrees that a lot of ore deposits are controlled by lineaments which reflect fault and fracture networks.

Anyhow, it seems to have become a conventional view that, if taken in combination with other geological methods and applied with precaution, the technique might provide a researcher with new kind of valuable information which would have remained hidden otherwise. This study takes into consideration only lineaments and their distribution, without preliminary geological/geophysical/geochemical data analysis.

All lineaments were divided (ranged) into four groups - main, secondary tertiary and circular. The drawing has been done in ArcGIS environment in real coordinate world. When necessary, the source images were georeferenced using ArcMap Tools, as well as other georeferencing software.

Tertiary lineaments can be seen as straight lines due to changes in surface pattern or color nuances in the images (Figure 2). The length of tertiary lineaments is usually in the range of 1/100-1/20 (with few outliers shorter and longer) of the area of the study size. Sometimes, substantial portions of the areas under the study are covered with cultivated fields, residential areas and roads. Drawing the tertiary lineaments in these areas is impossible, and roads/power lines etc. must not be mixed up with natural lineaments. Such areas are either excluded from tertiary lineament analysis or are considered with particular precaution during the interpretation.

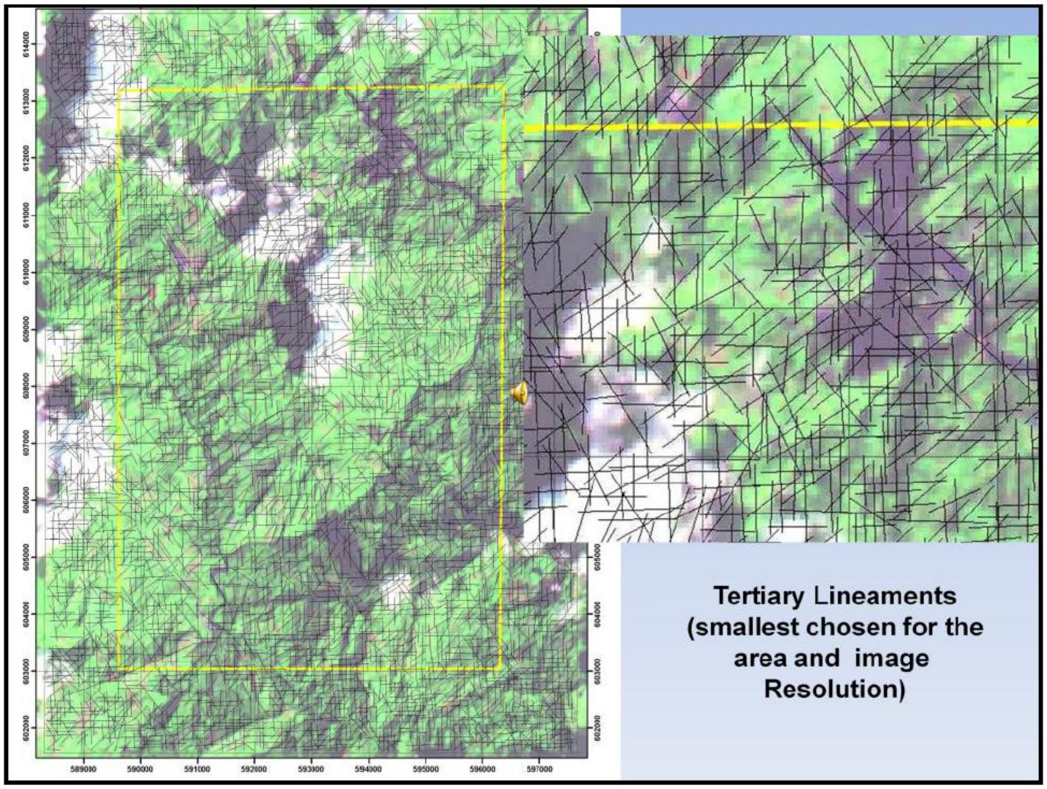

Figure 2. Tertiary lineaments.

Secondary lineaments (Figure 3) can be seen as straight lines due to changes in surface pattern or color nuances extended through several hundred meters. The length of tertiary lineaments is usually in the range of 1/20-1/5 (with few outliers shorter and longer) of the area of the study size.

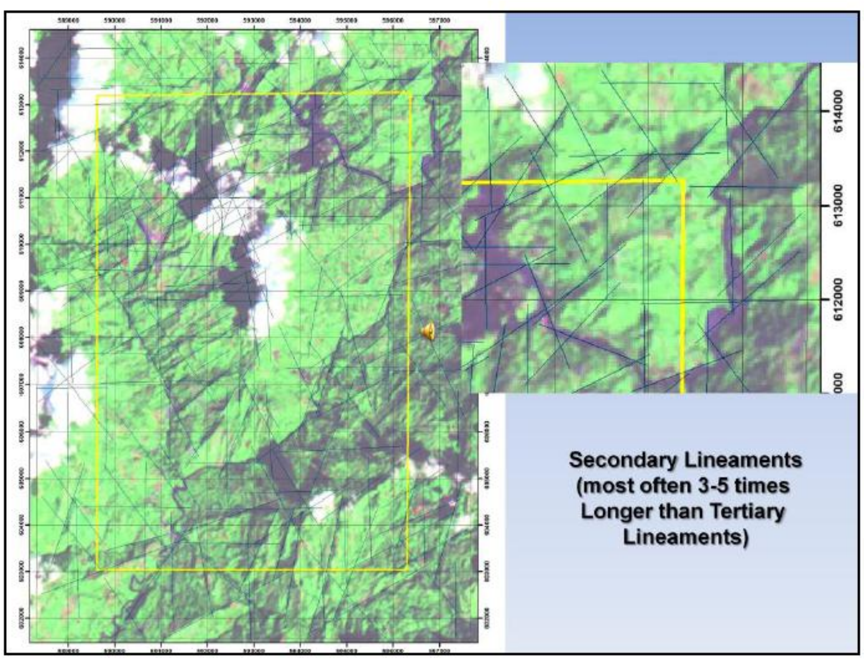

Figure 3. Secondary lineaments.

Main lineaments can be clearly traced through at least 1/3 of a map or longer and often may be represented as series of closely placed parallel lineaments (Figure 4).

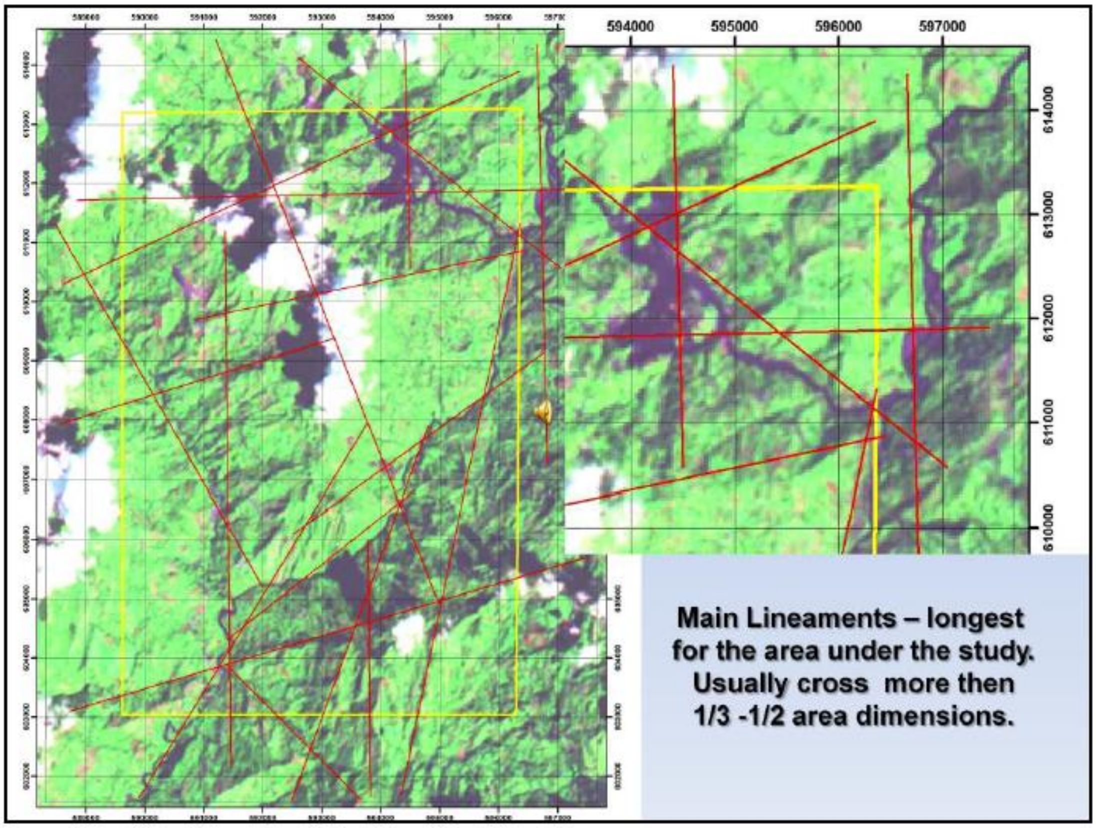

Figure 4. Main lineaments.

Circular lineaments (Figure 5) can be seen and drawn using both the colour changes and the pattern. Circular lineaments played an important role in this study. Their diameter varies broadly.

Circular lineaments in some cases may be divided into two-three scale groups by their diameter.

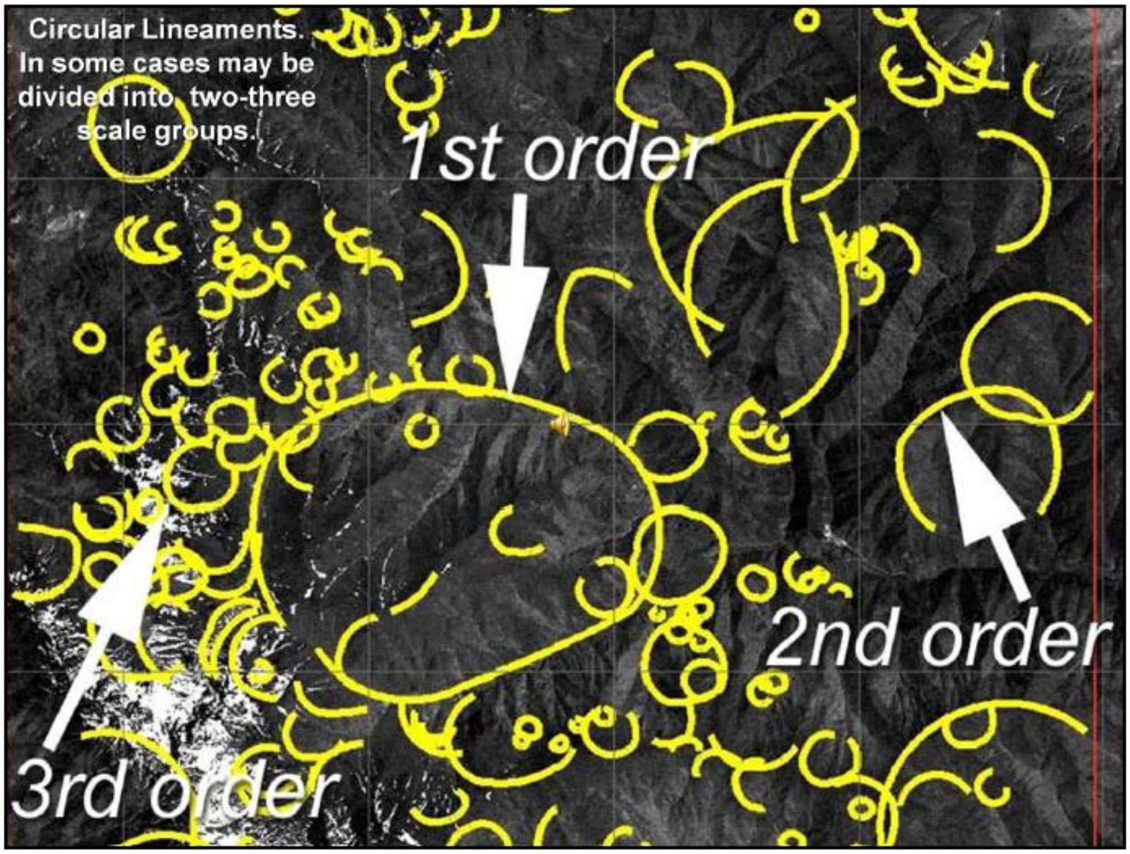

Figure 5. Circular lineaments.

It is important to note that the lower limit for the lineament's length (minimal length of tertiary lineament) is scale dependant. The image with 0.3-1.3 m/pi resolution allows seeing and drawing very short lineaments – 4-5 m long. The number of the features to draw would become enormous - hundreds of thousands and/or millions. Since the analysis is done manually, it would take several months of work for one person, which is unreasonable. That is why the researcher should spend some time just evaluating the right scale with which to start.

The total number of different groups of lineaments, and the number intersections between each type of the main 4 groups of lineaments are calculated and exported as an Excel file (Figure 6).

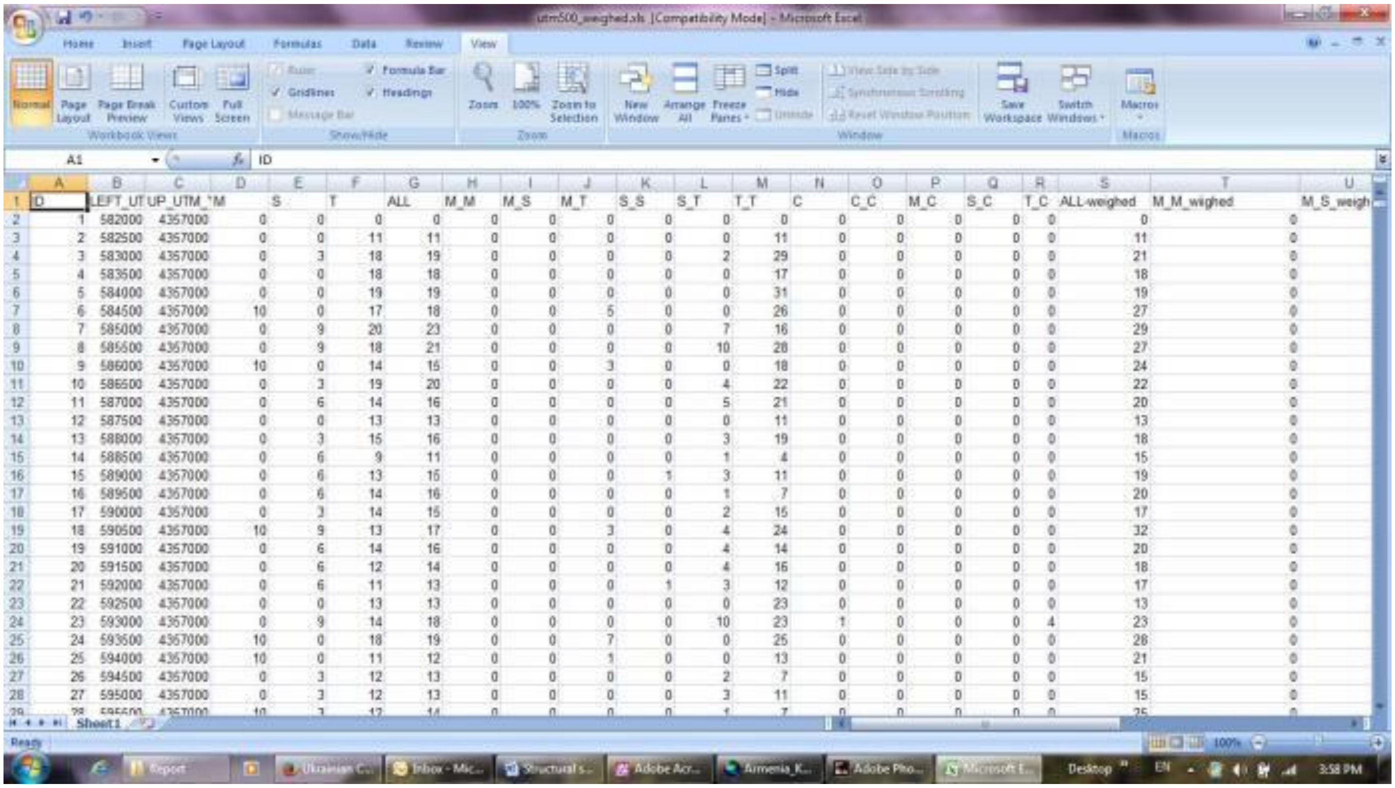

Figure 6. Calculation and weighting the lineaments.

Calculation and interpretation was done with specially designed software written for ArcView 3.2 using different averaging window size. In this study we used

The table data then was processed and interpreted with the Surfer software. We used Krigging method for gridding; the resulted maps are contour maps of lineament (lineament intersections) densities. The maximums on such maps represent the areas with the highest lineament population (density), and therefore, with the highest permeability for any fluid flow passing through the system. Apparently, an amount of fluid flowing through the zone with maximum lineament (intersections) density is larger with comparison to the minimum, and the mineralization is more likely to occur in the maximum density zone.

We also used some weighting procedure during the interpretation.

Weighing is somehow arbitrary and reflects the researcher's conception of the lineaments nature and origin. From mechanical standpoint fractures and faults (which we observe as lineaments) form in some hierarchic order, usually from the smallest – first in time, and then to the largest. Again, mechanically-wise, the fracture's shape in the homogeneous body must be close to a square or disc. So, the lineament, say, 200 m long may cut into the rock down to approximately 200 m, and the main lineament 6 km long¸ accordingly, to 6 km down. Such a conception may be an oversimplification, yet the tendency of the longer and wider lineaments to penetrate deeper than shorter ones is a well established geological fact.

Apparently, an amount of fluid flowing through the main lineament is larger with comparison to the tertiary ones, and the mineralization is more likely to occur in the vicinity of the main lineament. Therefore, it makes sense to weigh (assign the *importance* value) the main lineament heavier than secondary, and much higher than tertiary. In our processing we used the following weighting coefficients: tertiary – 1, secondary – 3, main – 10, circular -10. The intersections, accordingly, became weighted, since the weighted numbers for different groups changed. In the areas where the mineralization is controlled, to some extent, by intrusive magmatism and volcanism it is reasonable to weigh the circular structures heavier than small linear features. These circular structures may reflect location of eroded intrusive bodies, volcanoes or their translucent projections onto the surface.

By the same token, though, if the geological data suggest that the mineralization occurs at shallow depth and related to, say, rather small intrusive bodies, then the role (weight) of tertiary/secondary lineaments and their intersections would be more important (heavier weight). Since this study does not involve geology/geophysics/geochemistry consideration in detail, we will show contour maps built with different weighing procedures.

From general considerations the locations with maximal densities of lineaments/intersections will be considered as the most favorable for mineralization to occur, since those areas must have the highest permeability for circulating fluid.

Application of different averaging window sizes gives some ideas about the regional significance of the max/min density zones. Sometimes, when moving from smaller to larger averaging window size the maximums disappear and/or shift to another location. In such a case one can reasonably assume that the maximums reflect the very local (and relatively shallow) structural situation. As often, though, the maximums stay at the same location, just growing in size. Such a pattern suggests the existence of deeper and more regional source of the tectonic disturbance in the area. Again, depending on the geological model accepted for the mineralization in the study area, either smaller or larger window results may be chosen as more important from the exploration standpoint.

The pattern and the spatial distribution of zones with different lineament densities are really important. Lineament analysis does not give the exact targets for immediate drilling, rather provides some clues for further ground exploration.

Contour maps from Surfer were exported into ArcMap 10.6.

An important question should be discussed with regard to maximum cut-offs. The method is not intended to obey to strict statistical rules. And every region is geologically unique. Same can be said about the lineaments. Their distribution can be fairy even, and in such a case the min-max values of their densities won't be of a huge difference. The cut-offs, say, 60-75% of the max value (or even higher) could be appropriate to map the maximums. As another extreme – the lineament distribution can be very uneven, and cut-offs of 30% of max value can be used. We do not want the maximum to be neither too small-size nor too large. In the first case, one cannot be absolutely sure that there was no error made during the manual procedure of drawing or during the processing. In the second case, one can obtain maximums (targets) which cover more than 50% of the area, and that definitely would not make sense from the exploration standpoint. So, the mapping of the maximums is a compromise between the statistics and practicality. Understanding of this issue becomes particularly important when we walk down the size of the averaging window. The smaller the size the more cautious one will have to be sometimes in terms of choosing the cut-offs.

It is obvious that the weighting procedure makes sense only when we consider more than three different groups of the lineaments together. Clearly, if we look only at, say, secondary and main and tertiary lineaments intersections, the spatial distribution of the maximums will stay the same regardless of the maximums magnitudes (Figure 7).

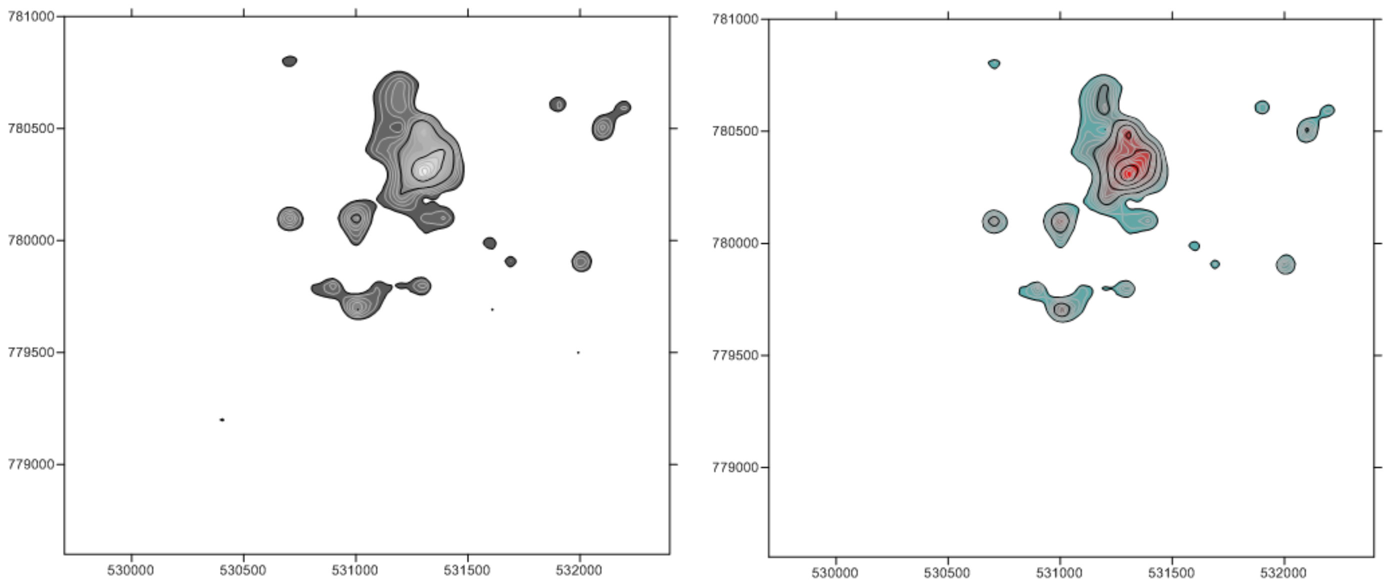

Figure 7. Maximums of secondary and tertiary lineaments intersections densities – weighted (left) and unweighted (right)..

There is no point in showing all the possible combinations of the contour maps. There are too many of them to put into comprehensive Report. Any combination and consecutive contour maps can be easily produced with common contouring software (Surfer, ArcMap etc.). Tables of lineaments of different averaging windows for such procedure are provided in Digital Delivery Package accompanying the current Report.

All the maps have many common features. By overlaying all the individual maps and extracting areas where several individual maps maximums intersect we obtain the most probable “Target Exploration Maps.

As we already mentioned, the detail data coming from other sources and of different nature are not used at this stage of the method application. Due to this, we cannot choose “the most correct” map for exploration purposes, neither we must be in a favor of an “averaged” scheme. The next necessary step would be the testing the obtained maps against the geology/geophysics/geochemistry, ongoing data collection, or/and field testing of the lineament anomalies.

If one of the maps proves to be the best with regard to new flow of the collected data, then we can use such a map as an exploration tool for the future work planning.

We must emphasize that the smaller the size of the window as compared to the size of the area under the study, the less reliable become the exact spatial positions of the maximums and their absolute magnitudes, since the number of secondary, main and circular lineaments is not usually statistically large for such a window. Still, with cautiousness, the results can be very useful in combination with other data. Any particular area usually has its specific "ideal" averaging window size.

Physical Modeling

Main earth crust and/or uppermost mantle heterogeneities (such as deep faults and fault zones as well as favorable pattern of faults and their intersection) are considered to be the locations of magma generation and penetration, sedimentary basins development, high permeability zone formation, metamorphic processes and fluid flow canalization. The last two lead to remobilization and re-precipitation (redistribution) of ore, oil, gas etc.

Spectrum of deposit types that are mainly controlled by faults geometry and pattern is extremely wide ranged – from diamonds and PGM to oil and gems.

It would seem to be simple, then, at least at a first glance, to design some structural exploration method: one must find and outline all major faults in the area of interest, outline zones of maximal faults densities and "knots" of fault intersections, and these resulted spots should be the most favorable for deposit finding.

There are, though, two problems for this procedure to be easily fulfilled.

First problem. It is not always possible to establish all major faults at once, especially when one studies an area with an overburden or just because of absence of any reliable geological data.

Second problem. Theoretical considerations as well as the experimental results and a geological practice indicate that only a few among many faults (fractures in experimental works) and their intersections play controlling role in deposit location whereas others serve either as pathways for deposit mass supply or don't affect geological system at all. This phenomenon becomes clear from the following simple experiment which everyone can reproduce at leisure time.

Let us take a rubber eraser and make several cuts on one of its facets (Figure 8). Then, press eraser from two sides horizontally. You will immediately see that openings form along some cuts (which are parallel or close to parallel to the direction of compression) whereas other cuts do not manifest themselves. Now try to press eraser in different direction, bend it, twist it, and play with it around. You will find a number of deformational patterns, yet initial system of cuts is the same. This experiment gives may be too general, yet a good analogy of faults /strain field interaction in nature (cuts represent faults and strain field - pressure applied by your fingers).

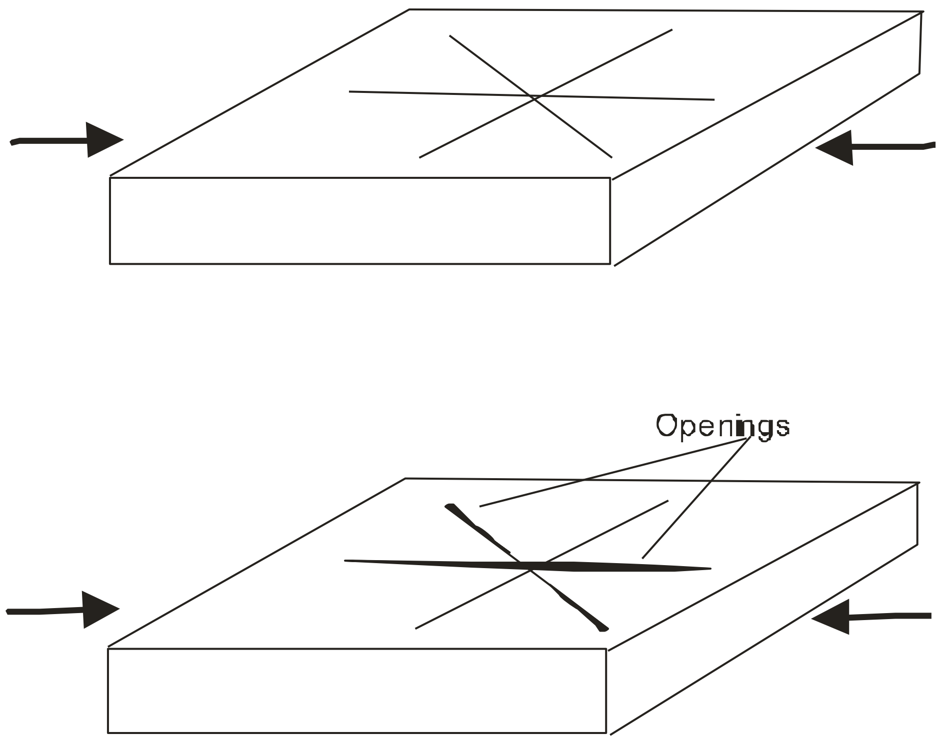

Figure 8. Faults behavior due to compression orientation.

The First problem can be solved by lineament analysis of relief, air- and satellite images, radar images, geophysical fields etc.

Lineaments are superficial “traces” of buried faults, and their visibility even through hundreds of meters of overlaying sediments is well explained from the mechanical standpoint. Many specialists in mechanics believe that any fault with substantial length (say, 2 km) behaves as a very mobile structure, since even in a dormant tectonic environment cumulative stress on it happens to become greater than the average strength of rocks. Once formed, such faults manifest themselves in tiny movements which are not significant in magnitude but still keep the faults active. These continuous movements can be seen through later structures as lineaments – faults or fracture zones with constant, often pendulum-like (pulsating) type of little displacements.

Thorough lineaments analysis and subsequent processing of lineament data allows us to find the most important (main) structures which control the system mechanical behavior.

Yet, to overcome the Second problem (see above) and find which high fracture density zones must be explored first and foremost we have to do some additional discriminative analysis. We need to select those faults and their intersections, those high fracture density zones which were the most geologically active and dominant in the area under study. There is no way to crack this problem theoretically since the real faulted volume behaves as a non-linear system for which mechanical equations proved to be insoluble.

There is, nevertheless, a way around, namely, tectonophysical (physical, analogue) modeling.

Physical modeling deals with simulation of real geotectonic processes by using analogue materials instead of rocks, and substituting natural tectonic stresses, temperatures and pressures by specifically selected laboratory conditions. While deforming selected models with initial fault structures again and again, one has to register all newly formed strain structures (usually with digital camera) and, then, analyze dozens of images to select and outdraw repeating zones of high strain.

Many-year experience of research indicates, that no matter what orientation of stress and what materials one chooses, he will always find only a few of such zones of highest strain with astonishingly stable spatial location!

These zones in experiments and their analogues in nature, called structural (tectonic) concentrators, indicate the most favorable localities for any type of mineral deposit.

Some preliminary words need to be said about the physical modeling foundations relevant to the case-study:

Analogue modeling is a simplification of Nature; using this method, structures formed due to the deformation of rocks can be modeled and investigated. The history of physical (tectonophysical) modeling goes back at least 130 years (Figure 9). Cadell was one of the first known to make a model of faults and folds using simply sand and clay. Today we still use this technique to investigate relations between for instance material properties and geological (tectonic) deformations of different scale.

Figure 9. Cadell's experiments.

Cadell (in 1886) turns the handle to move the wall to the left which cause the sand and clay to be compressed. The result explains the structures he has observed in the field. (Source: https://virtualexplorer.com.au/article/2002/48/thermomechanical-analogue-modelling/paper1.html).

Physical modeling deals with simulation of real geotectonic processes by using analogue materials instead of rocks, and substituting natural tectonic stresses, temperatures and pressures by specifically selected laboratory conditions.

Our lack of knowledge about "real" rocks is one of the major limitations to any kind of modeling of deformation. However, unlike their counterparts in Nature, the initial (undeformed) stages of analogue models can be documented, and can easily be compared with their later, deformed stages. This comparison is essential to gain an understanding of the evolution of the resulting structures. Analogue modeling is a relatively simple and inexpensive technique which can be very valuable as long as its limitations are well understood.

Basically, tectonic deformation, as any deformation, consists of three consecutive stages: elastic (reversible), plastic and rapture (permanent, irreversible). When the plastic stage is short in time and insignificant in magnitude we usually describe the deformation as brittle – it occurs under relatively low temperature and/or high stresses and high strain rate.

During all these stages in the heterogeneous geological media (faults are the most important of heterogeneities) mineralization tends to localize in the (or close to) zones of low compressive and/or high tensional stresses. Generally speaking, we may say that mineralized fluids move from zone of high compressive stresses into zones of openings (raptures, fractures, faults) and low compressive (or high tensional stresses) where they precipitate and form ore bodies.

Thus, if we use physical modeling to allocate the most favorable zones for deposit discovery we have to find zones of: high rapture deformation or, in other words, zones with high density of fractures and openings – so called 'dilation (dilatation) zones', or in the areas of relatively low compressive stress compared to adjacent high-stressed zones.

To cover all three stages of deformation in experiments we have to use two **different types of materials** (these are just technical aspects of the modeling and won't be discussed here) and, therefore, two **different series of experiments** have to be conducted: *elastic deformation* (reversible) and *plastic + rupture deformation* (irreversible).

Geological deformations either have occurred or could have occurred many times in the past, under different thermodynamic and tectonic conditions. That is why we **need to study separately several (namely, twelve) stress/strain regimes** – group of mainly "pure shear" with four different orientations of compression and group of mainly "simple shear" with four different orientations of shearing.

Figure 10 shows the general setup for 12 experiments (12 different stress/strain orientation axes) used in series of plastic and elastic experiments:

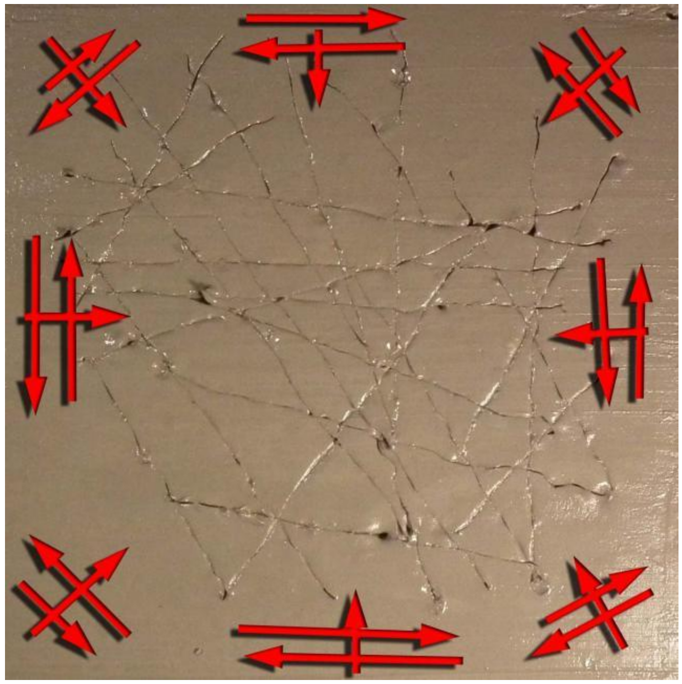

Figure 10. 12 plastic/elastic deformation regimes. Principal model.

<u>Plastic Modeling</u>

The model itself is made with clay dope whose mechanical properties satisfy, in general, the demands of *The Theory of Similarity* for this class of analogue modeling.

In the clay block with dimensions 20x20x2.5 cm a series of vertical cuts is made. These cuts represent main lineaments (faults) obtained from lineament analysis of the satellite images. The same fault-template is used in all experiments, yet its orientation relative to stress varied in each case.

Mainly Pure Shear Group (Figure 11). Mechanical sketch of this situation may be represented as follows.

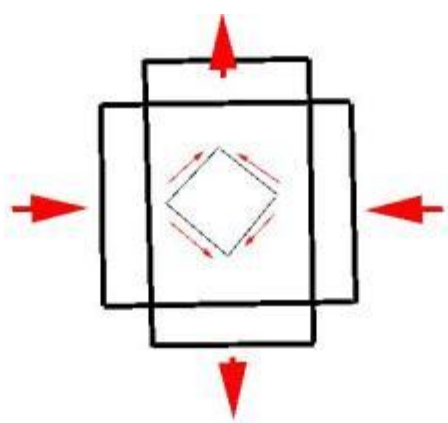

Figure 11. Sketch of the mainly pure shear group of deformation.

Mainly “Simple Shear” Group. Mechanical sketch of this situation may be represented as follows (Figure 12).

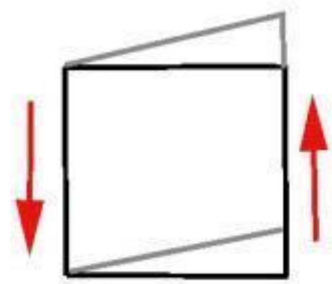

Figure 12. Sketch of the mainly simple shear group of deformation.

Simple shear is considered as an ideal situation which is seldom to exist in earth crust, some kind of trans-pressure (additional compression perpendicular to red arrow on the Figure 12 above) or trans-tension occurs usually. In our experiments such additional shortening was at a range of 10-20%.

The results of experiments are recorded with digital camera, and images are interpreted separately. Zones of openings along existing faults as well as new fractures and areas of high plastic deformations were outlined. Due to large distortions of initial pattern of faults during the deformation we copied these contours to the initial template and corrected their position to match with real lineaments pattern.

Zones of openings along existing faults as well as new fractures and areas of high plastic deformations are outlined. Due to large distortions of initial pattern of faults during the deformation we copied these contours to the initial template and corrected their position to match with real lineaments pattern.

All contours of high deformations in eight experiments are overlaid in one picture, and divided into four districts of strain level was made as following:

1-white - zones of zero strain – no strain was recorded in all experiments.

2-blue – zones of weak strain – strain was recorded in only one experiment

3-yellow- zones of medium strain – strain was recorded in 3-4 experiments

4-red - zones of high strain – strain was recorded in 5 or more experiments.

Finally, the table of strain intensity was made, with the following values for strain levels:

zones of zero strain -0

zones of weak strain – 1

zones of medium strain – 3

zones of high strain – 10.

For those cells which contained several areas of different strain-levels, simple weighting was applied.

Some emphasis must be put on the interpretation of the results. In our view, actual location of zones of high strain (and, thus, of high possible permeability and destruction of rocks) should be obtained from lineament scheme. In case of mismatch of lineaments densities and high-strain zones locations an additional consideration from regional geology data must be taken into account for one to decide which result should overrule the other. In other words, final targets must not be selected based on quantitative coefficients only.

Elastic modeling

Photoelasticity is an experimental method to determine the stress distribution in a material.

The name photoelasticity reflects the nature of this experimental method: *photo* implies the use of light rays and optical techniques, while *elasticity* depicts the study of stresses and deformations in elastic bodies. Through the photoelastic-coating technique, its domain has extended to inelastic bodies, too.

Photoelastic analysis is widely used for problems in which stress or strain information is required for extended regions of the structure. It provides quantitative evidence of highly stressed areas and peak stresses at surface and interior points of the structure — and often equally important, it discerns areas of low stress level.

The method is mostly used in cases where mathematical methods become quite cumbersome. The method serves as an important tool for determining the critical stress points in a material and is often used for determining stress concentration factors in irregular geometries.

The method is based on the property of birefringence, which is exhibited by certain transparent materials. Birefringence is a property by virtue of which a ray of light passing through a birefringent material experiences two refractive indices. The property of birefringence or double refraction is exhibited by many optical crystals. But photoelastic materials exhibit the property of birefringence only on the application of stress and the magnitude of the refractive indices at each point in the material is directly related to the state of stress at that point. Thus, the first task is to develop a model made out of such materials. The model has a similar geometry to that of the structure on which stress analysis is to be performed. This ensures that the state of the stress in the model is similar to the state of the stress in the structure.

When a ray of plane polarized light is passed through a photoelastic material, it gets resolved along the two principal stress directions and each of these components experiences different refractive indices. The difference in the refractive indices leads to a relative phase retardation between the two component waves. The magnitude of the relative retardation is given by the *stress optic law:*

$$R = Ct(\sigma_{11} - \sigma_{22})$$

where R is the induced retardation, C is the stress optic coefficient, t is the specimen thickness, σ_{11} is the first principal stress, and σ_{22} is the second principal stress.

The two waves are then brought together in a polariscope. The phenomenon of optical interference takes place and we get a fringe pattern, which depends on relative retardation. Thus studying the fringe pattern one can determine the state of stress at various points in the material.

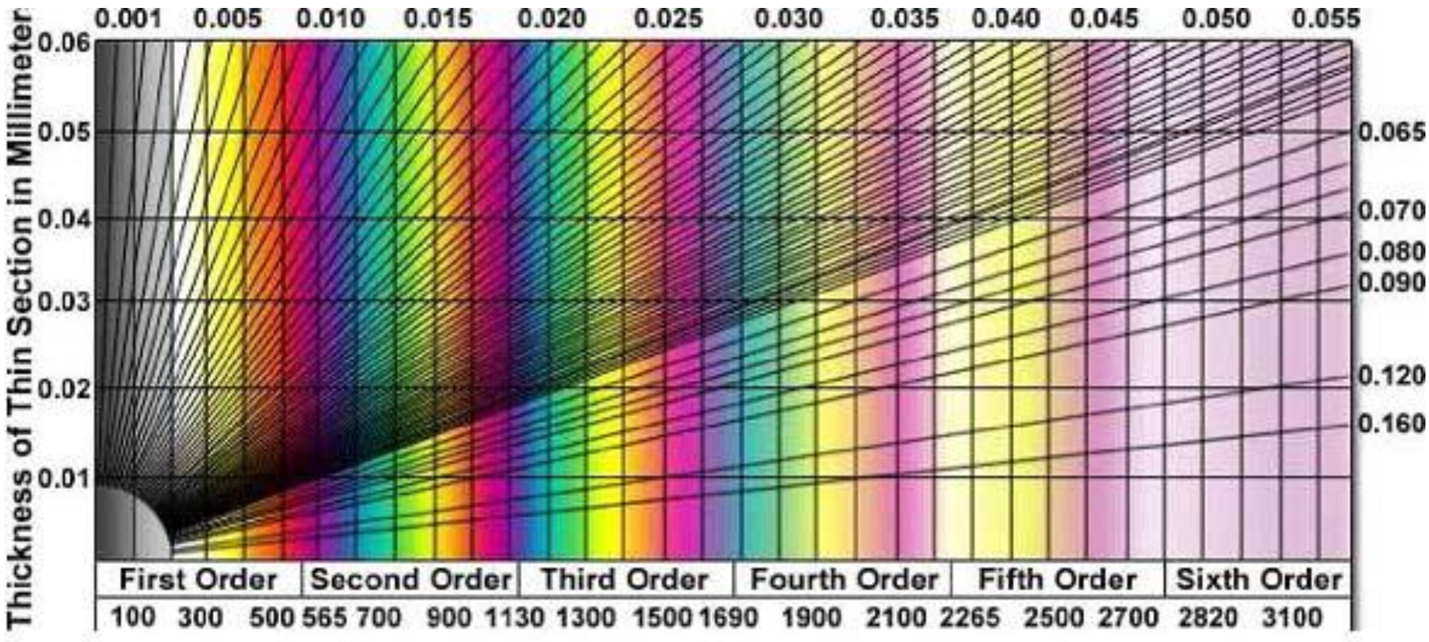

Fig 8. Michel-Levy interference color chart [1]

Figure 14. Michel-Levy interference color chart.

The birefringence of an anisotropic material can be estimated when observed and/or photographed in a Polariscope. A relationship between interference color and retardation can be graphically illustrated in the classical Michel-Levy interference color chart (Figure 14), presented above. This graph plots retardation on the abscissa and specimen thickness on the ordinate. Birefringence is determined by a family of lines that emanate radially from the origin, each with a different measured value of birefringence corresponding to thickness and interference color.

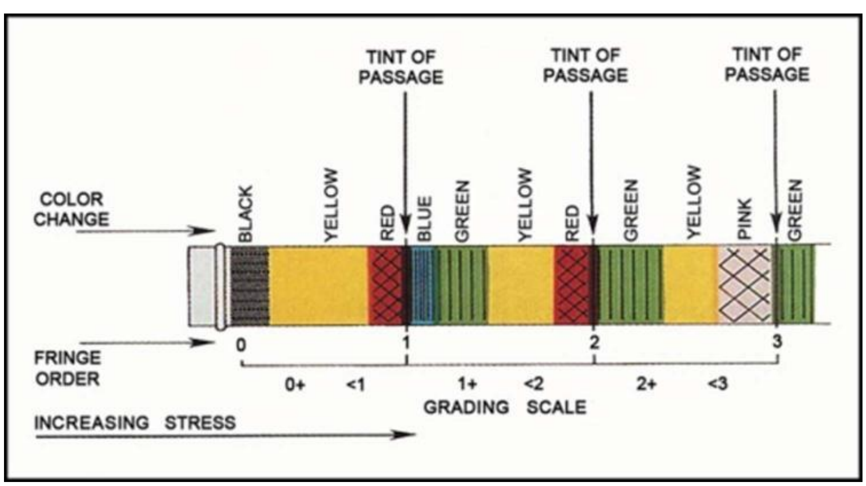

Figure 15. Colour chart.

For the purpose of our modeling we also use the chart in Figure 15. It shows the change in color due to increasing stress.

It is well known that in the elastic stress-field substances (fluid, mobile mineral components, magma etc.) move from the areas of high differential stress towards the areas of low stress. In the photoelastic modeling for the exploration targeting we are looking, therefore, for the low-stress areas and openings in the experiments.

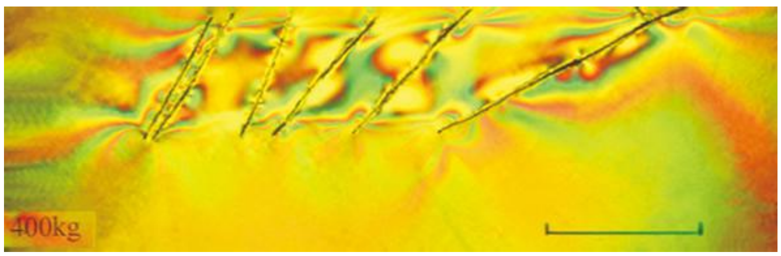

Figure 16. 400kg isochromatic graph of stress field of Luohu area in Shengzhen fault.

Figure 16 gives an example of one real regional study.

Gelatin is used as the optically active and most suitable materials for this type of modeling.
The device used for the modeling is shown in the Figure 17.

The gelatin sample is placed between two polarizing plates (perpendicular to each other) and put on the light table. The deformation is being applied to the sample, and the interference image is photographed.
For exploration purposes we should be interested only in relative spatial estimation of the stress level in the sample, so the actual values of the stress magnitude are not measured/calculated.

When all the experiments are done we outline the areas of high, medium and low stress/deformations for each of the experiments.

In practice, during the modeling we deal mostly with the colors of the 1st and 2nd isochromatic fringe orders; the low stress areas will manifest the colors from black to red of the 1st order and blue of the 2nd one, as it is shown in Figure . It is important to recognize whether the fringe order is increasing or decreasing along the path of the fringe count, and this skill is achieved with focus and practice.

Overlaying these patterns onto each other we usually find that in the model exist such zones where the deformation was high in more half (>6) cases out of all experiments.

These repeating zones of high fracturing and openings (traps) in the plastic/rupture series and zones of low stress (or openings) in elastic series both represent the most favorable places for the formation of ore deposits.

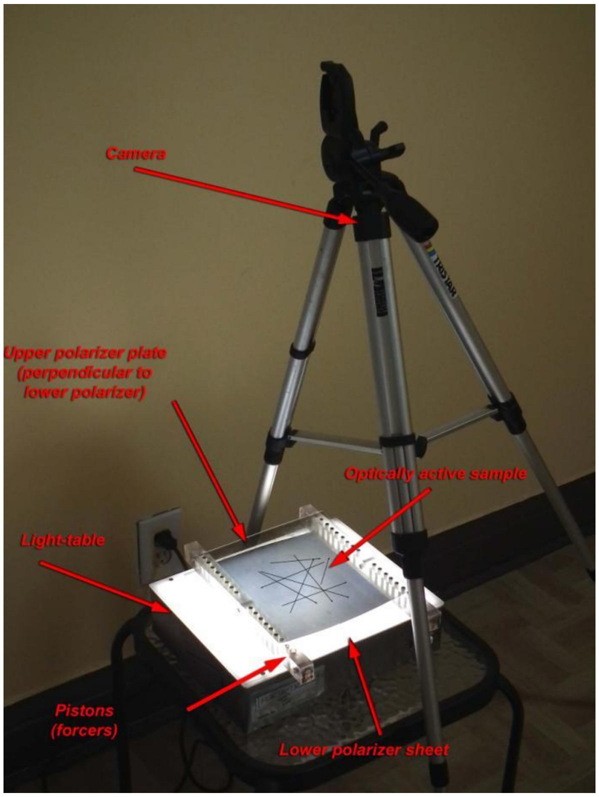

Figure 17. Elastic Modeling setup.

Although the results of physical modeling may be used for exploration targeting independently, it is better to use them as overlays over the results of lineament analysis. It is those locations where the highest densities of lineaments, lowest elastic strains and highest plastic/rupture strains come along that must be treated as the most favorable for any type of mineralization to occur.

Structural Lineament Analysis Application to Richmond Minerals Inc property, Huffman Twp. Property , ON, Canada.

Lineament Analysis of satellite and aerial photo images

For the analysis of the property (~4.8 sq km) the following 6 datasets were used:

- Lineament Analysis of the Bing satellite image (~ 1.54 m\px resolution – panchromatic, natural colour), (Fig. 18, a)
- Google Earth Image resolution (~ 2 m\px resolution, panchromatic, natural colour), (Fig. 18,b)
- Landsat image p021r027_7f20010929_z17_ps742.jpg (15 m/px resolution) – panchromatic (Fig. 18,c)
- Sentinel 2 monochromatic image – 10 m/px resolution - (Fig. 18,d)
- GRMT Topography (DEM) - ~ 2.5 m/px resolution -(Fig. 18,e)
- NASA_ASTER_USGS image - ~ 10m/px resolution - (Fig. 18,f)

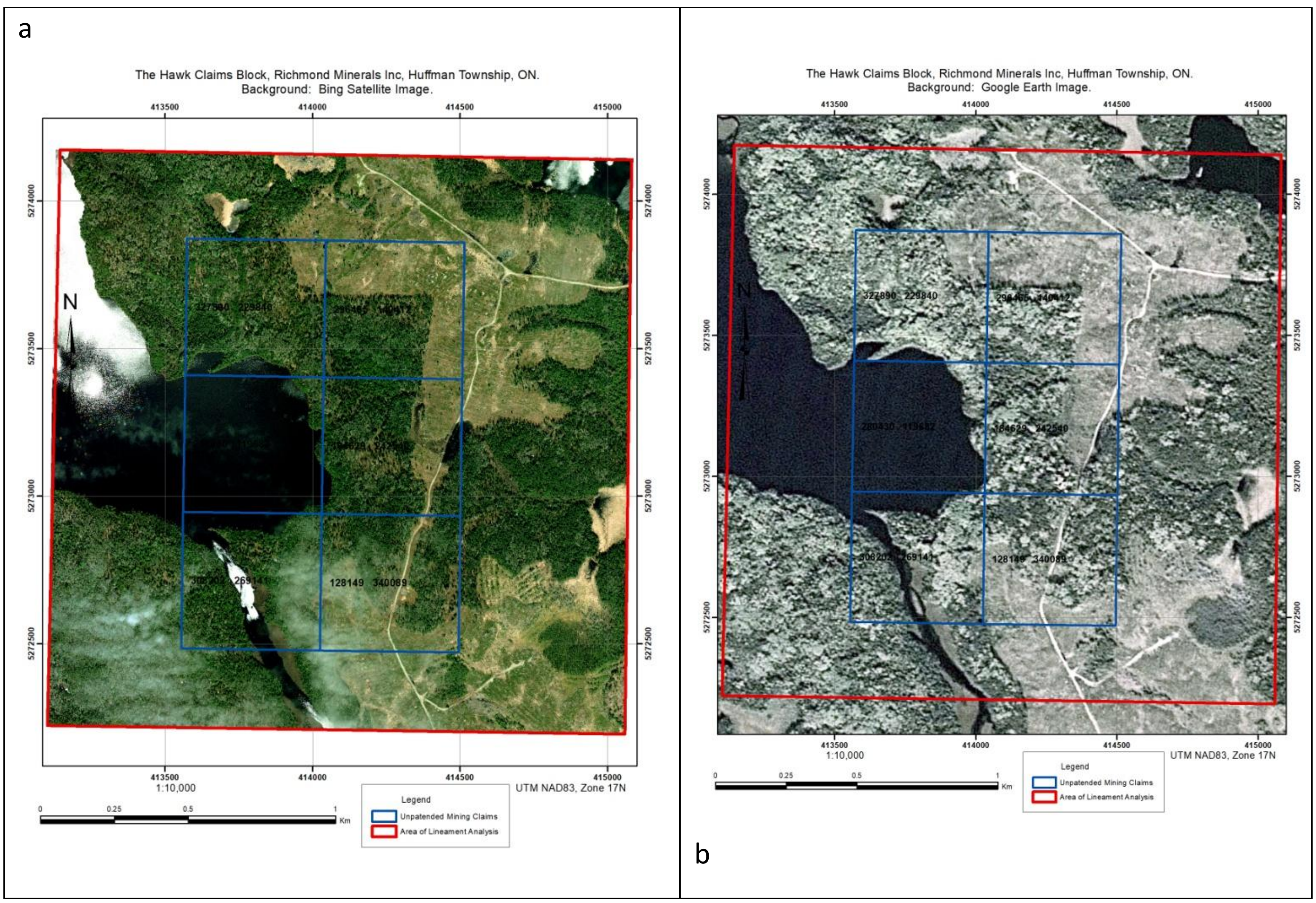

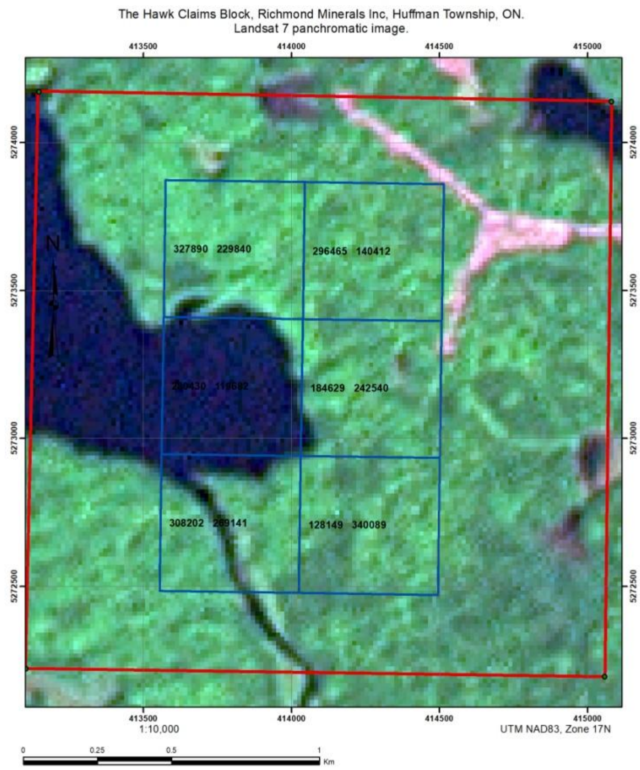
The Hawk Claims Block, Richmond Minerals Inc, Huffman Township, ON.
Landsat 7 panchromatic image.
413500
414000
414500
415000
5274000
5273500
5273000
5272500
N
327890 229840
296465 140412
184629 242540
308202 269141
128149 340089
1:10,000
UTM NAD83, Zone 17N
0
0.25
0.5
1
Km

c

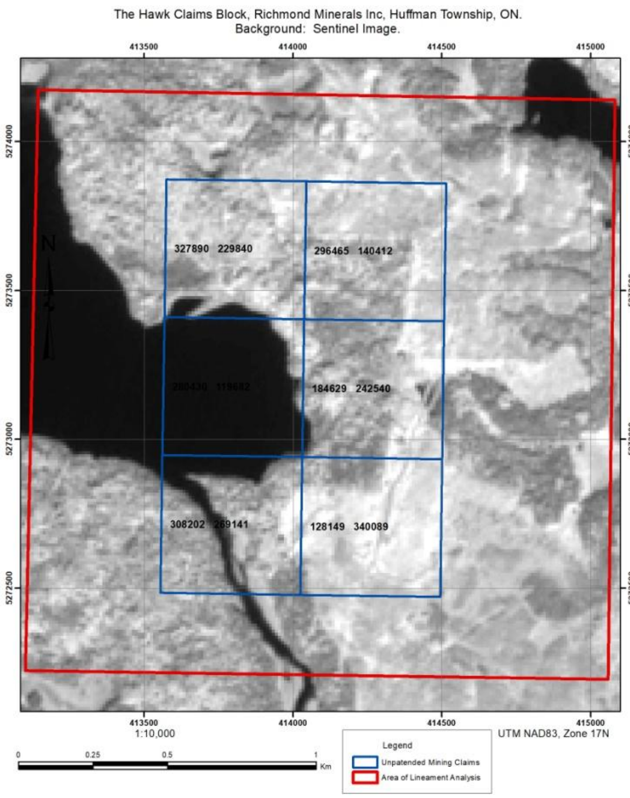
The Hawk Claims Block, Richmond Minerals Inc, Huffman Township, ON.
Background: Sentinel Image.
413500
414000
414500
415000
5274000
5273500
5273000
5272500
N
327890 229840
296465 140412
184629 242540
308202 269141
128149 340089
1:10,000
UTM NAD83, Zone 17N
0
0.25
0.5
1
Km
Legend
Unpatended Mining Claims
Area of Lineament Analysis

d

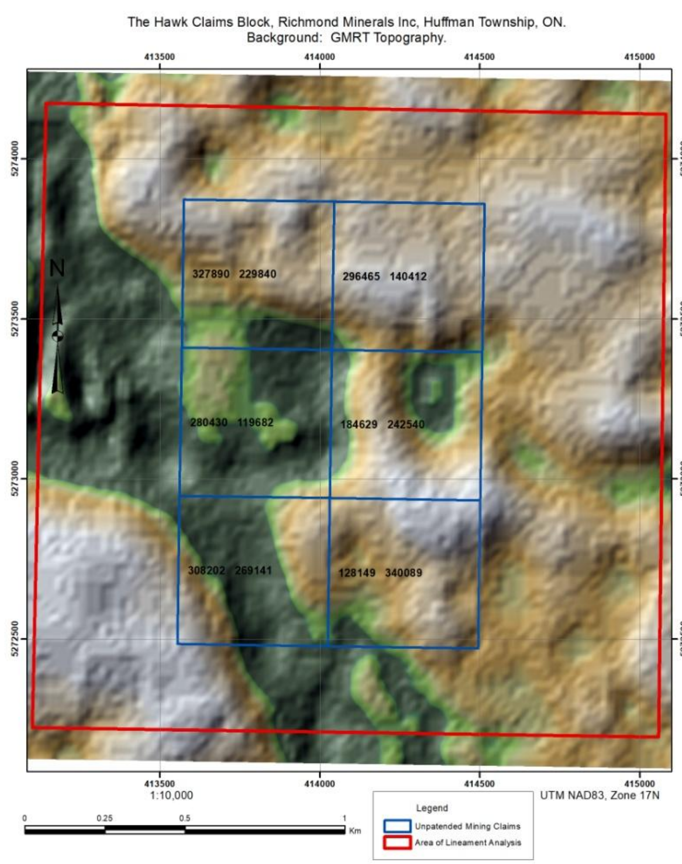
The Hawk Claims Block, Richmond Minerals Inc, Huffman Township, ON.
Background: GMRT Topography.
413500
414000
414500
415000
5274000
5273500
5273000
5272500
N
327890 229840
296465 140412
280430 119682
184629 242540
308202 269141
128149 340089
1:10,000
UTM NAD83, Zone 17N
0
0.25
0.5
1
Km
Legend
Unpatended Mining Claims
Area of Lineament Analysis

e

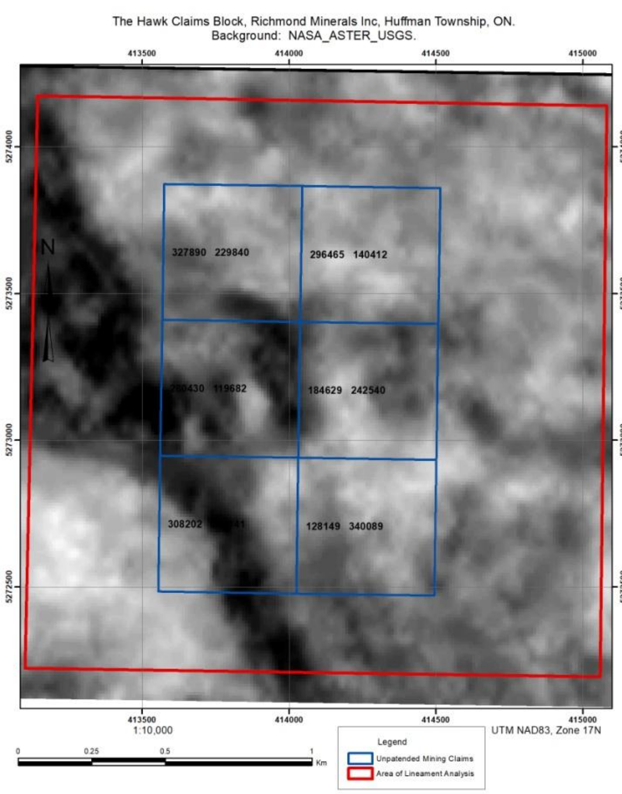
The Hawk Claims Block, Richmond Minerals Inc, Huffman Township, ON.
Background: NASA_ASTER_USGS.
413500
414000
414500
415000
5274000
5273500
5273000
5272500
N
327890 229840
296465 140412
184629 242540
128149 340089
1:10,000
UTM NAD83, Zone 17N
0
0.25
0.5
1
Km
Legend
Unpatended Mining Claims
Area of Lineament Analysis

f

The area is relatively small, and part of it is affected by economic activity. Although very high resolution image A27814_060 is available (~1 m/px resolution), it seems safer to start the lineament analysis with secondary level lineaments. Then, we can avoid the artificial linear structures as much as possible.

The following sets of lineaments were deciphered:

Secondary – length from **120** to (sometimes) **450** m. **941** secondary lineaments were identified. Notice, that Main lineaments may be represented as a chain of secondary ones; that is why (see below) main structures lines shine through the secondary lineaments -Figure 19.

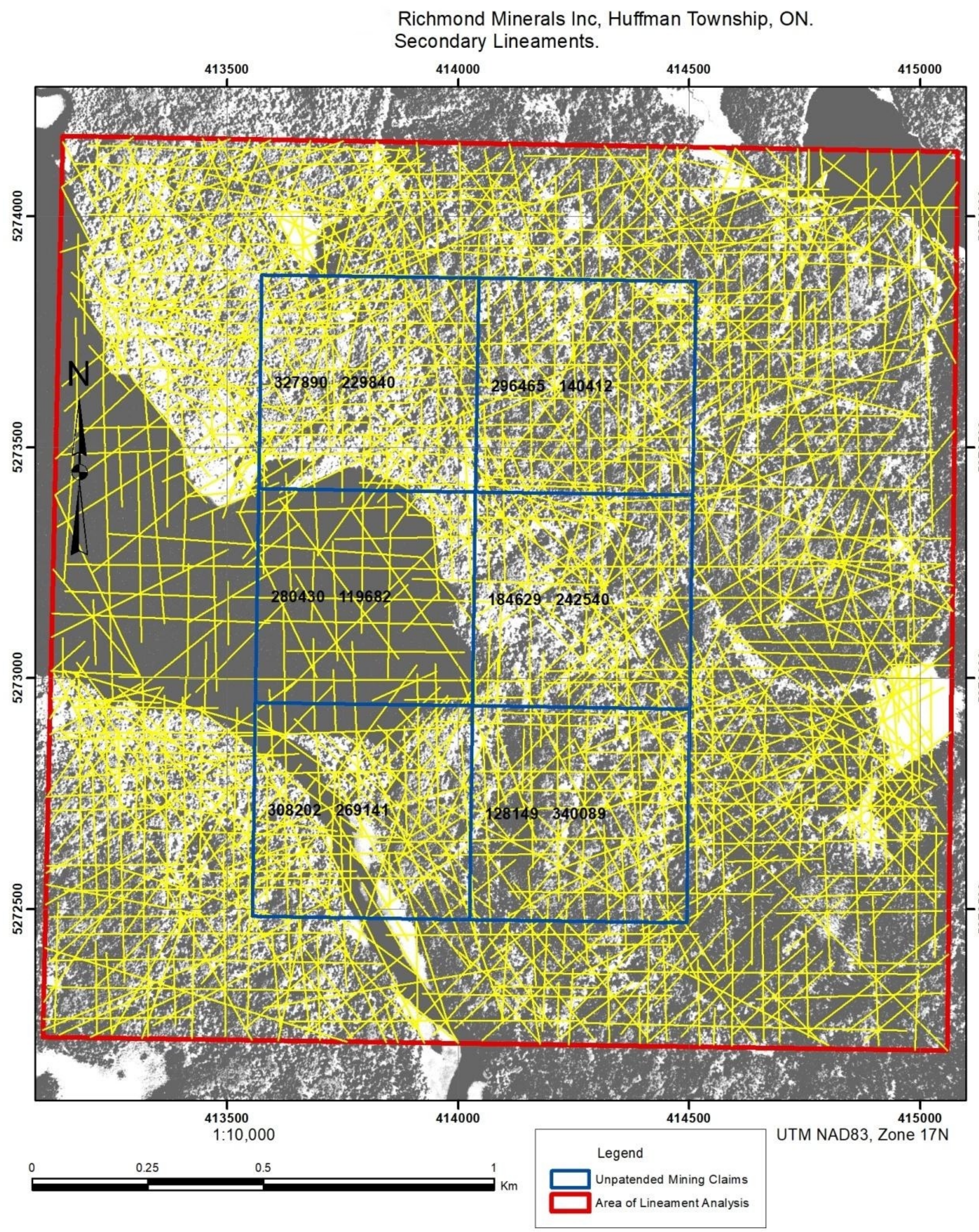

Figure 19 . Secondary lineaments, Huffman Twp. Property .

Circular lineaments (structures) – diameter from **50 m to 500 m, 21** structures identified - Figure 20.

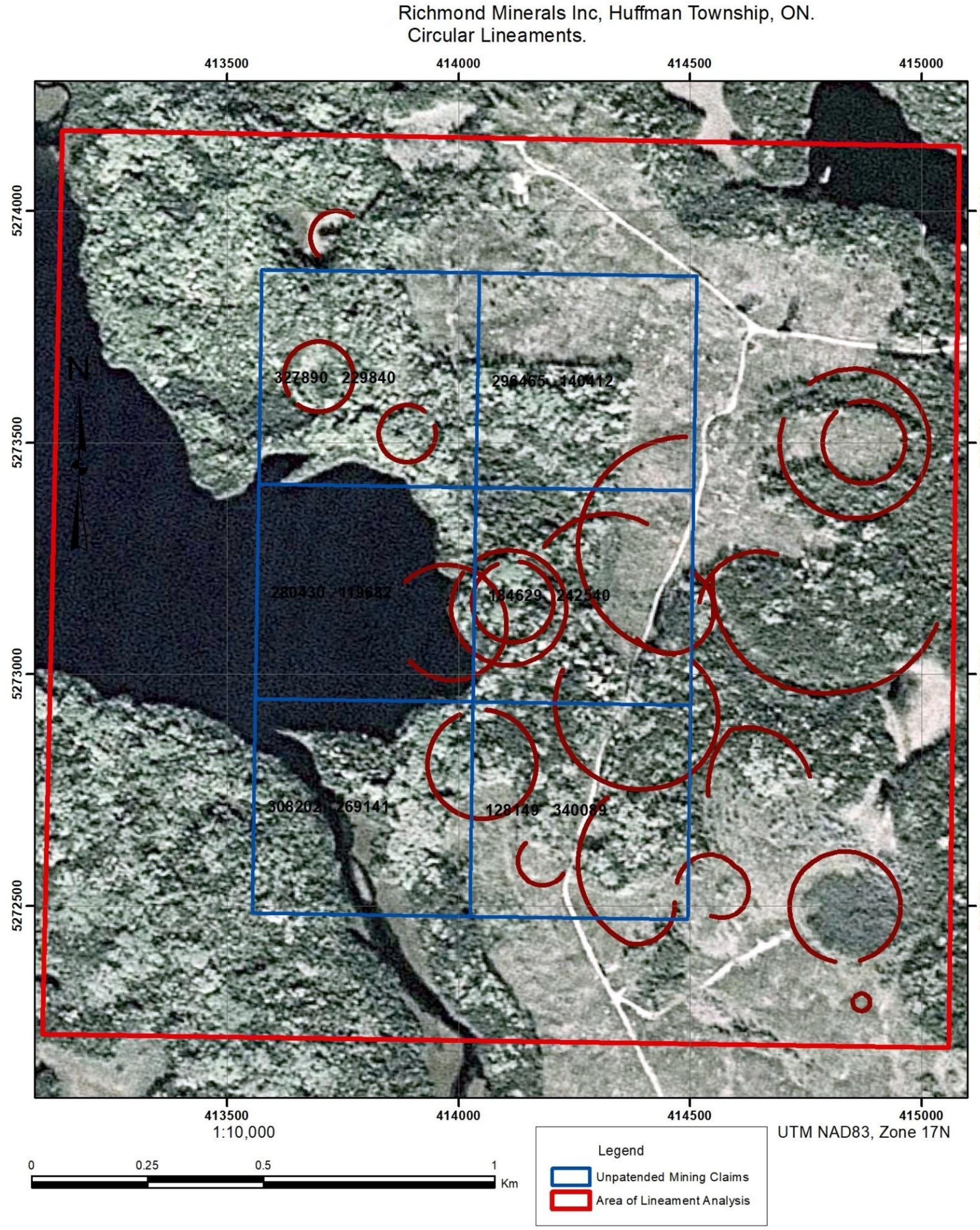

Figure 20. Circular lineaments, Huffman Twp. Property .

Main lineaments – longer than **1,300** m and up to 2,300 m , **23** lineaments identified. They may be used for the physical modeling along with property-scale faults – Figure 21.

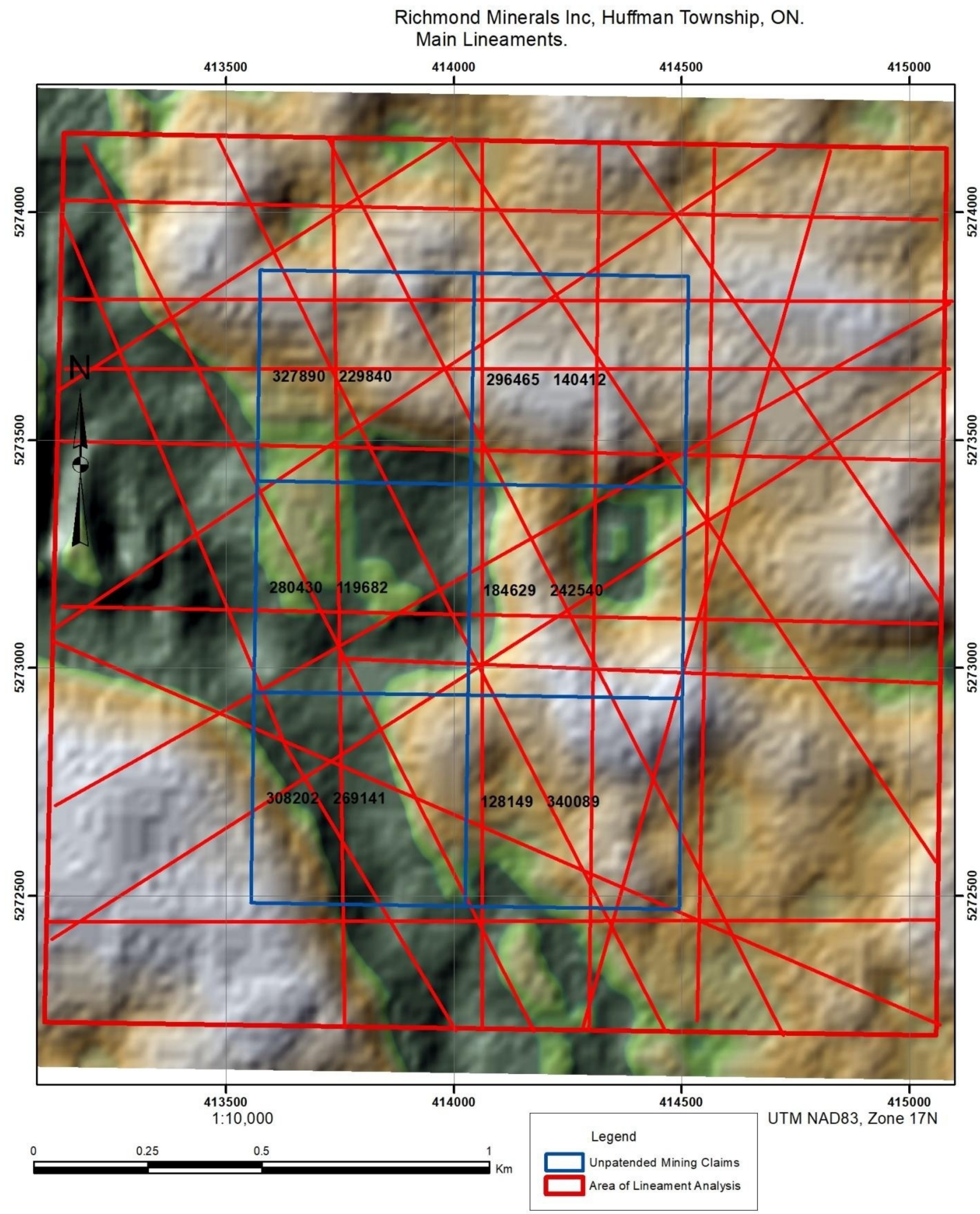

Figure 21. Main lineaments, Huffman Twp. Property.

Figure 22 shows all the lineaments on Huffman Twp. Property .

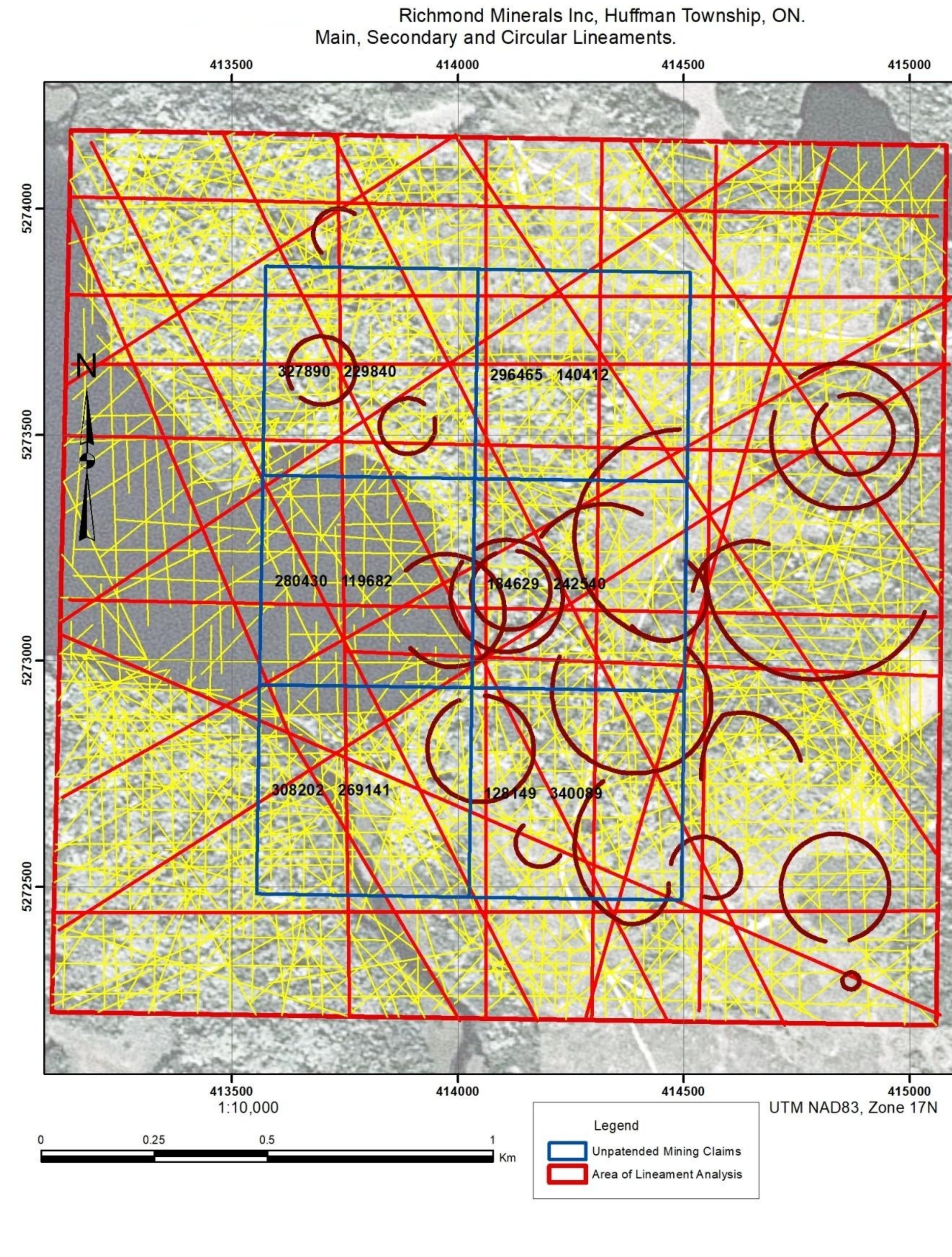

Figure 22.

Structural Lineament Analysis results processing with 100 m averaging window.

The following figures (Figures 23-29) show various maps depicting maximums of different groups of lineaments and their intersections.

Maximums of all lineamens densities (unweighed) on the Geological Map OFM 212. 100 m averaging window.
Richmond Minerals Inc, Huffman Township, ON.

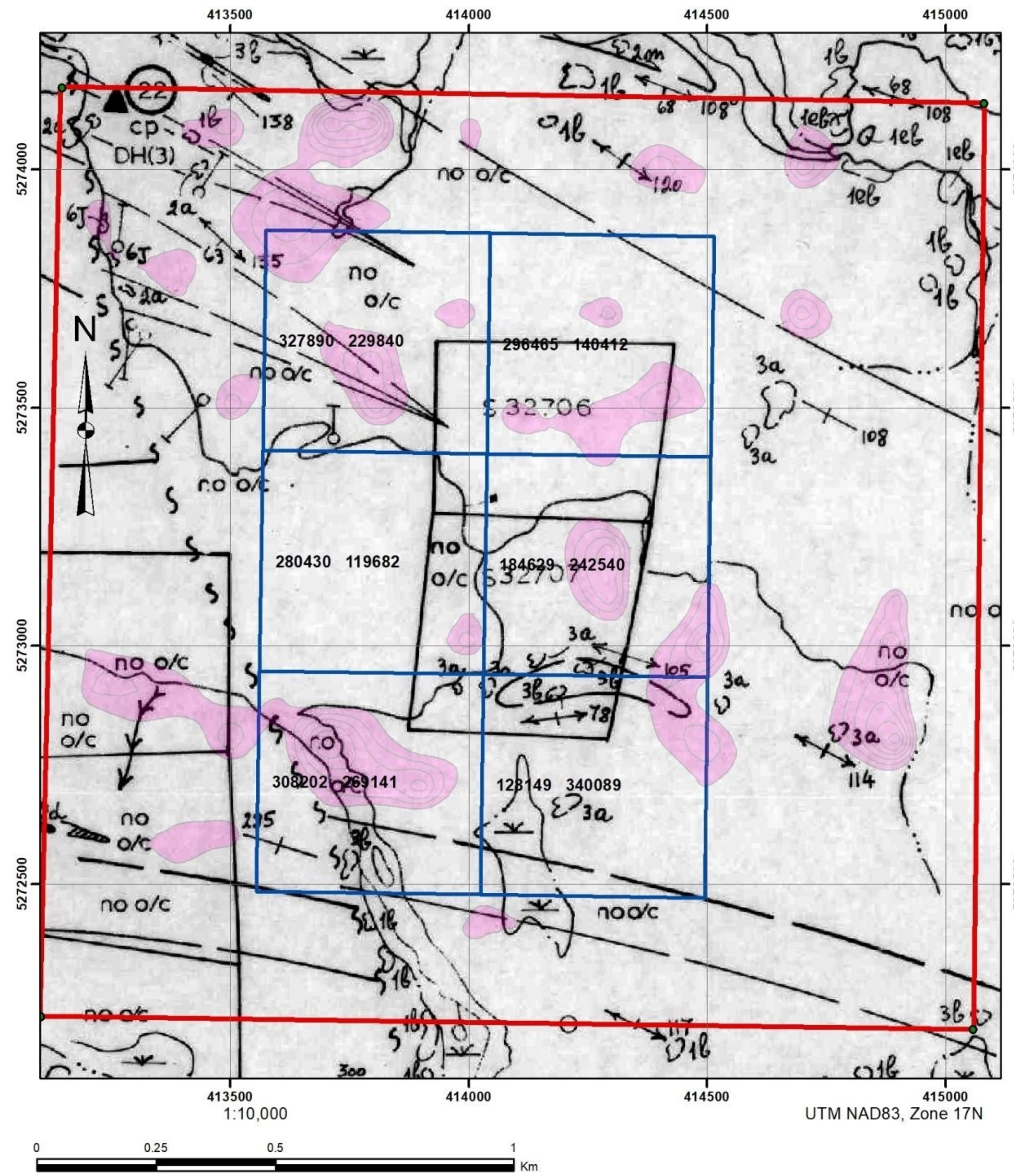

Figure 23

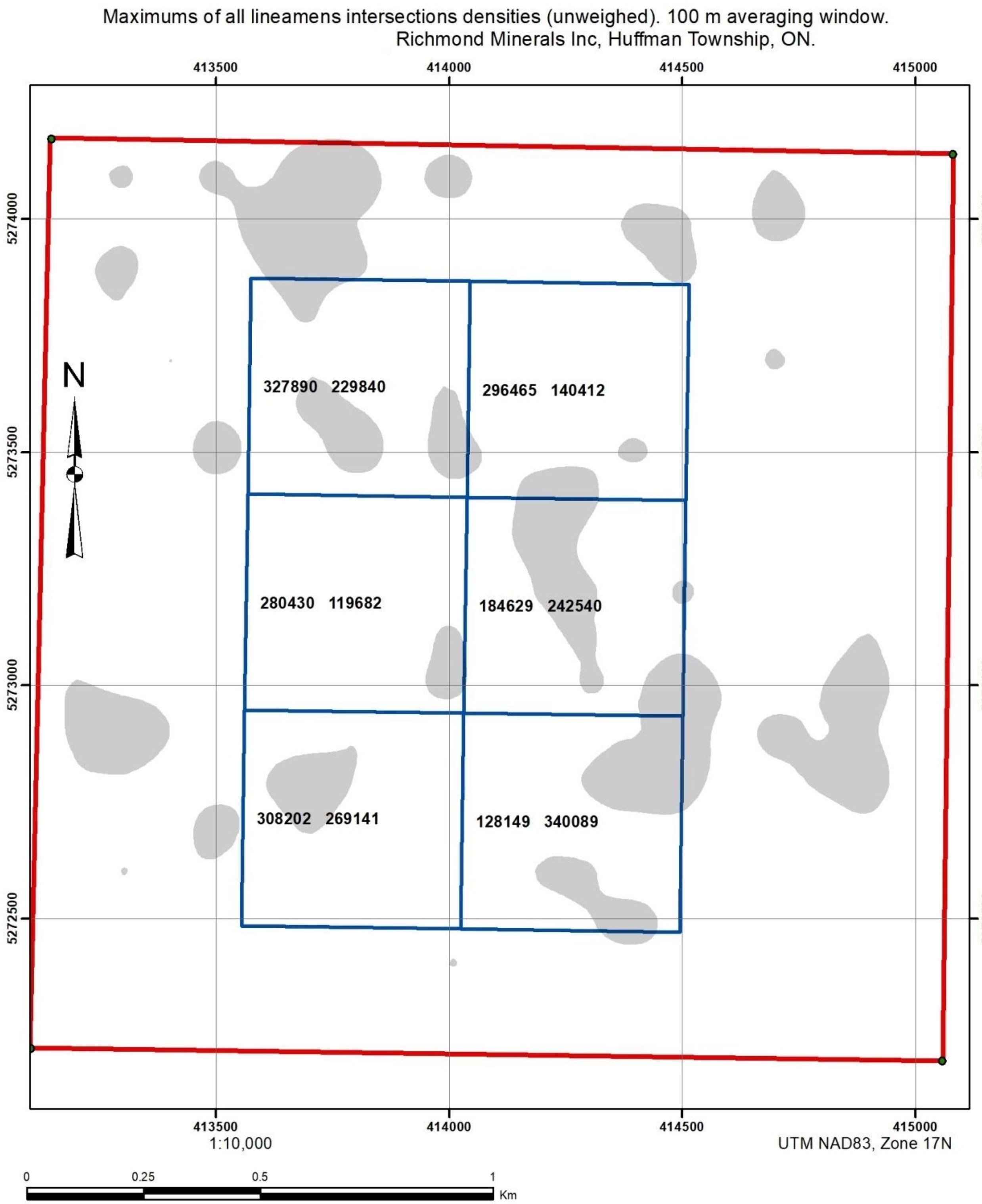
Maximums of all lineamens intersections densities (unweighed). 100 m averaging window.
Richmond Minerals Inc, Huffman Township, ON.
413500
414000
414500
415000
5274000
5273500
5273000
5272500
N
327890 229840
296465 140412
280430 119682
184629 242540
308202 269141
128149 340089
1:10,000
UTM NAD83, Zone 17N
0
0.25
0.5
1
Km

Figure 24

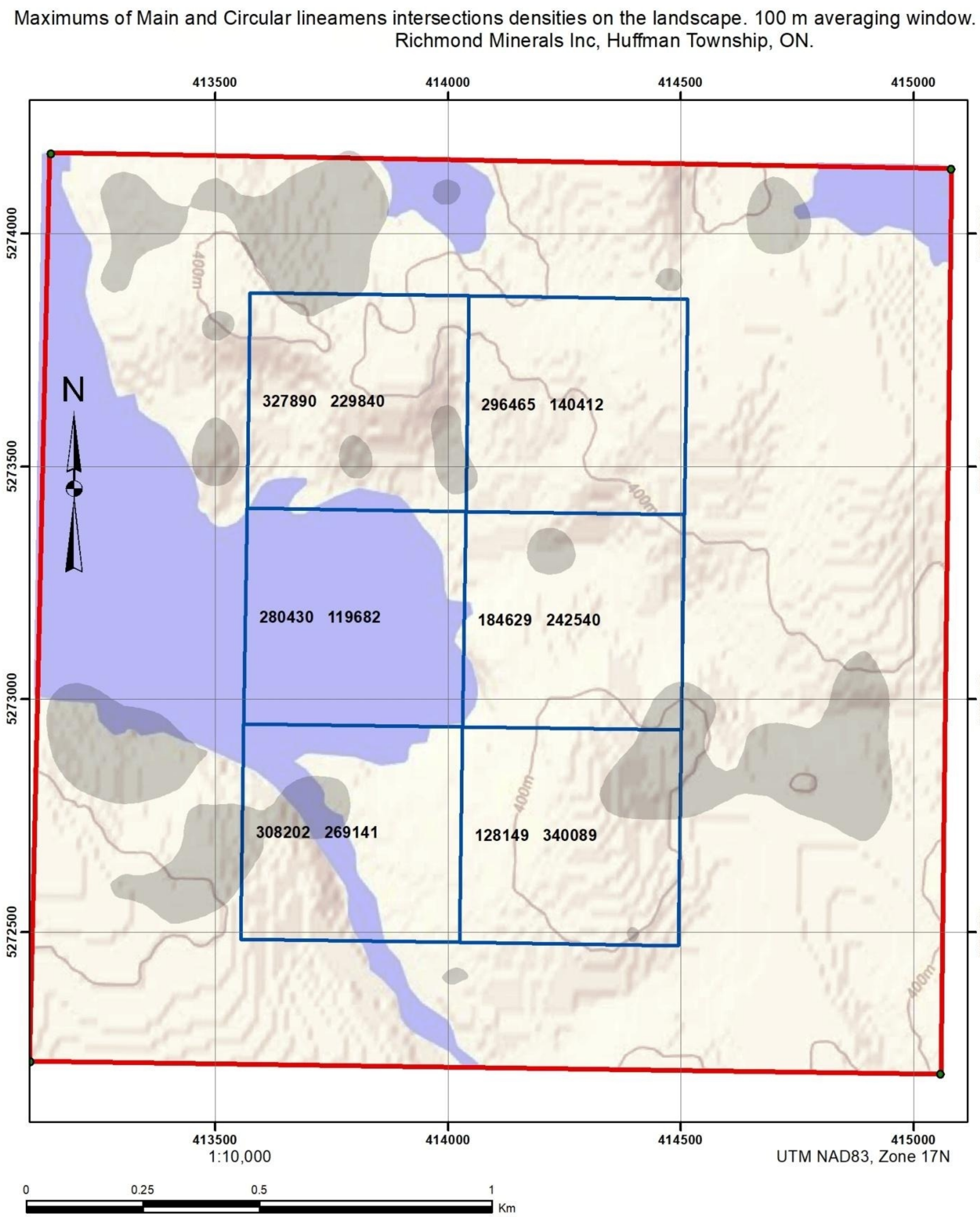

Maximums of Main and Circular lineamens intersections densities on the landscape. 100 m averaging window.
Richmond Minerals Inc, Huffman Township, ON.
413500
414000
414500
415000
5274000
5273500
5273000
5272500
N
327890 229840
296465 140412
280430 119682
184629 242540
308202 269141
128149 340089
400m
1:10,000
UTM NAD83, Zone 17N
0
0.25
0.5
1
Km

Figure 25

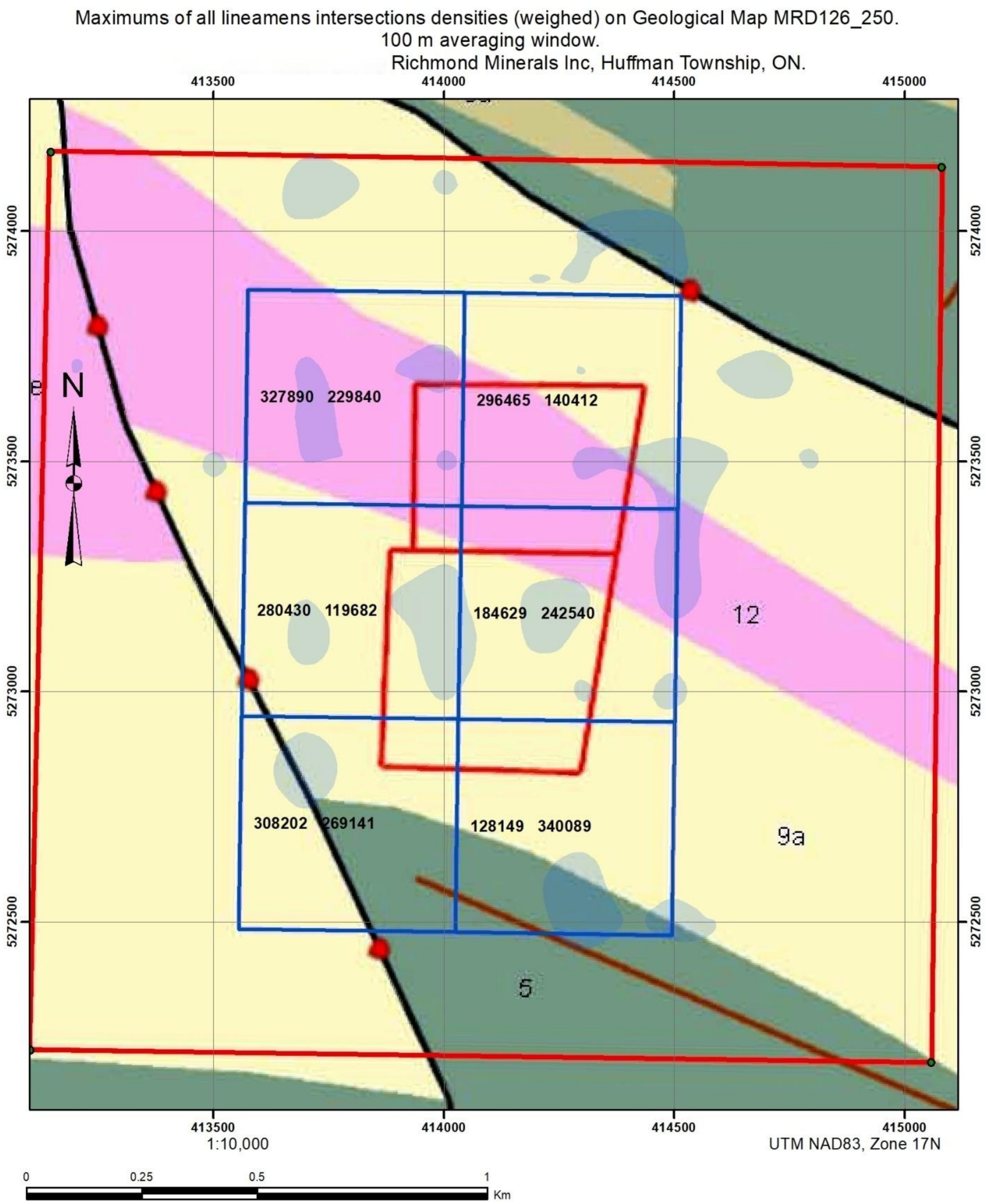
Maximums of all lineamens intersections densities (weighed) on Geological Map MRD126_250.
100 m averaging window.
Richmond Minerals Inc, Huffman Township, ON.
413500
414000
414500
415000
5274000
5273500
5273000
5272500
N
327890 229840
296465 140412
280430 119682
184629 242540
308202 269141
128149 340089
12
9a
5
1:10,000
UTM NAD83, Zone 17N
0
0.25
0.5
1
Km

Figure 26

Maximums of Secondary lineamens intersections densities on the landscape. 100 m averaging window.
Richmond Minerals Inc, Huffman Township, ON.

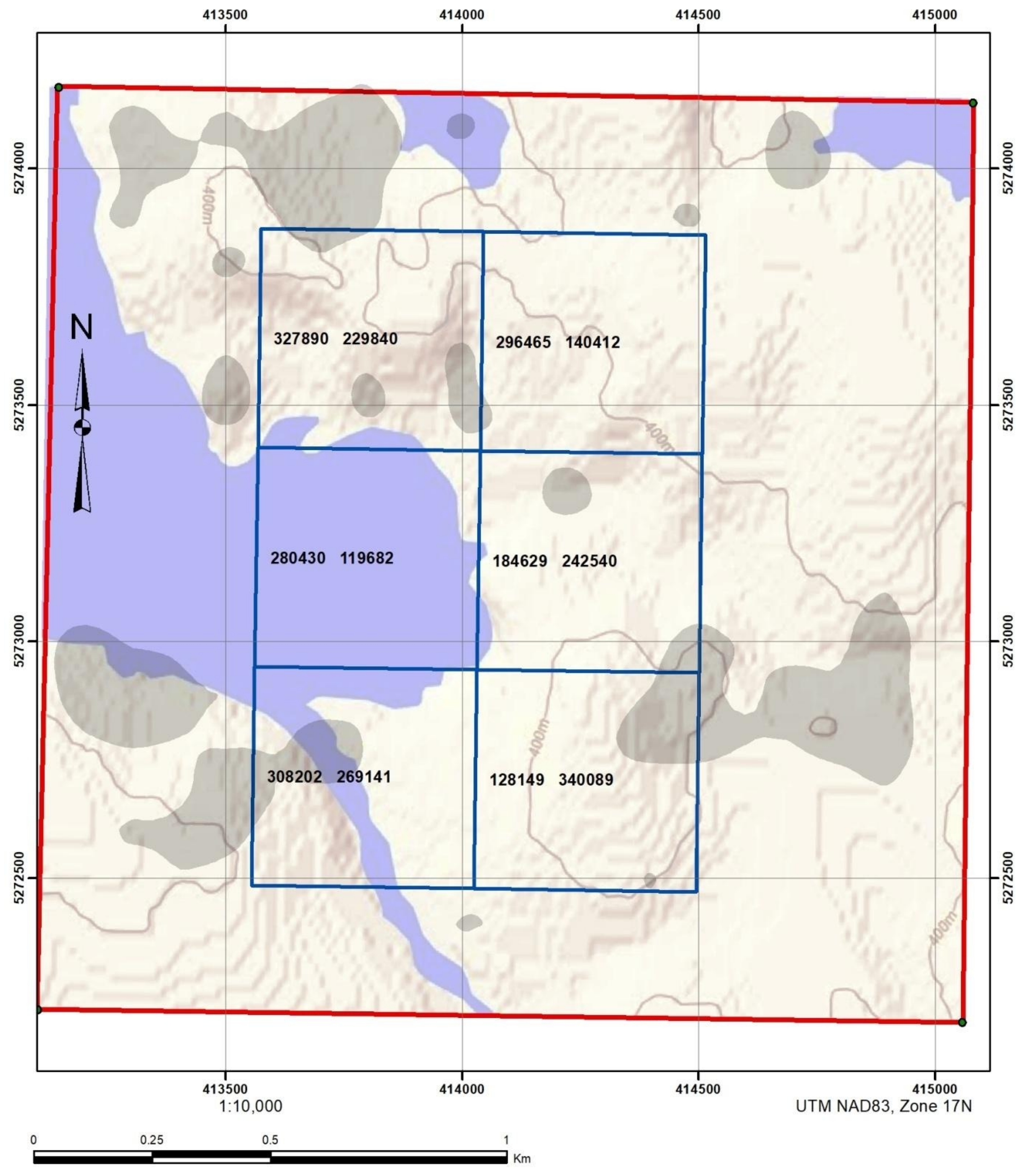

Figure 27

Maximums of Main and Secondary lineamens intersections (weighed) densities on the landscape.
100 m averaging window.
Richmond Minerals Inc, Huffman Township, ON.

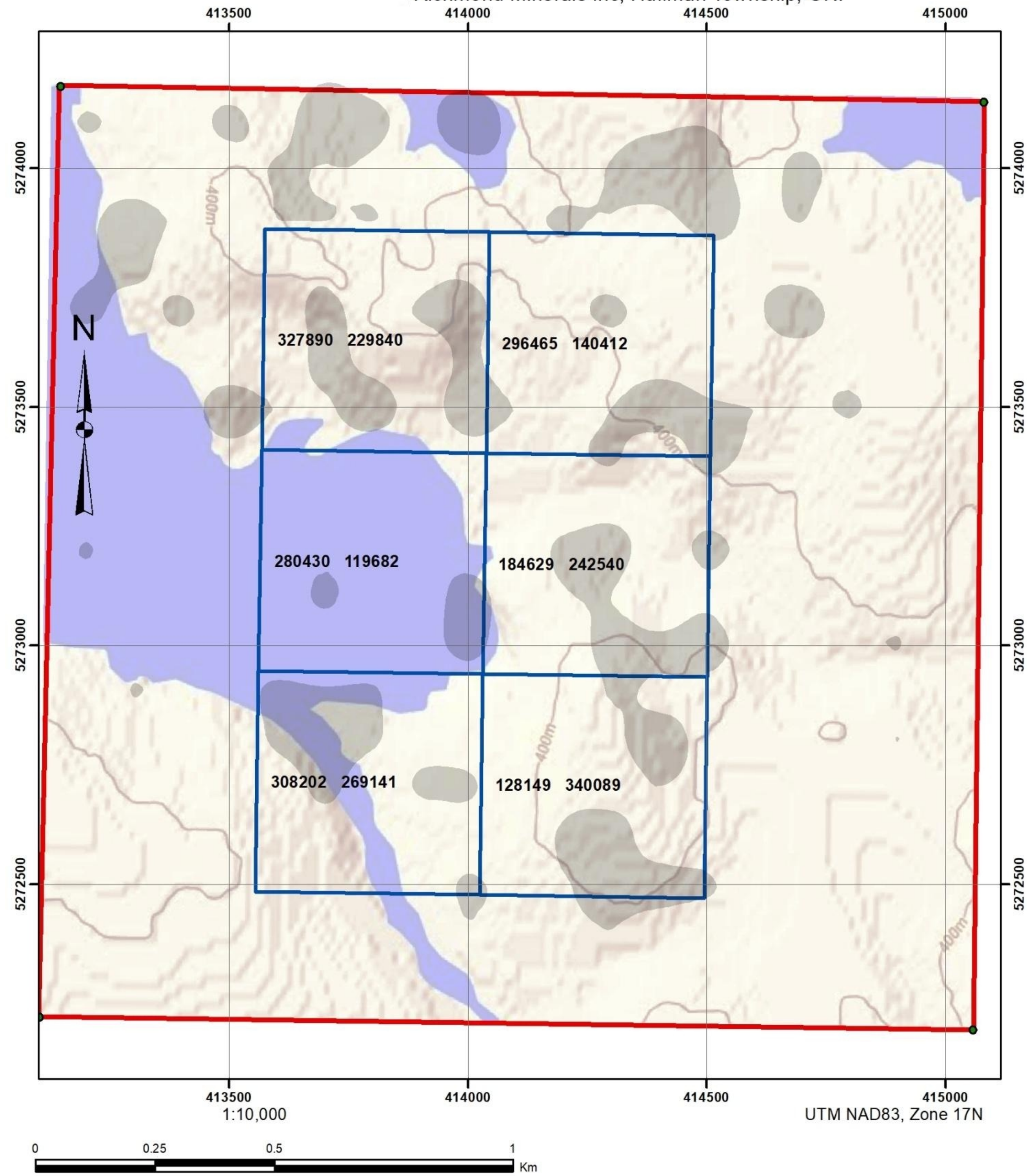

Figure 28

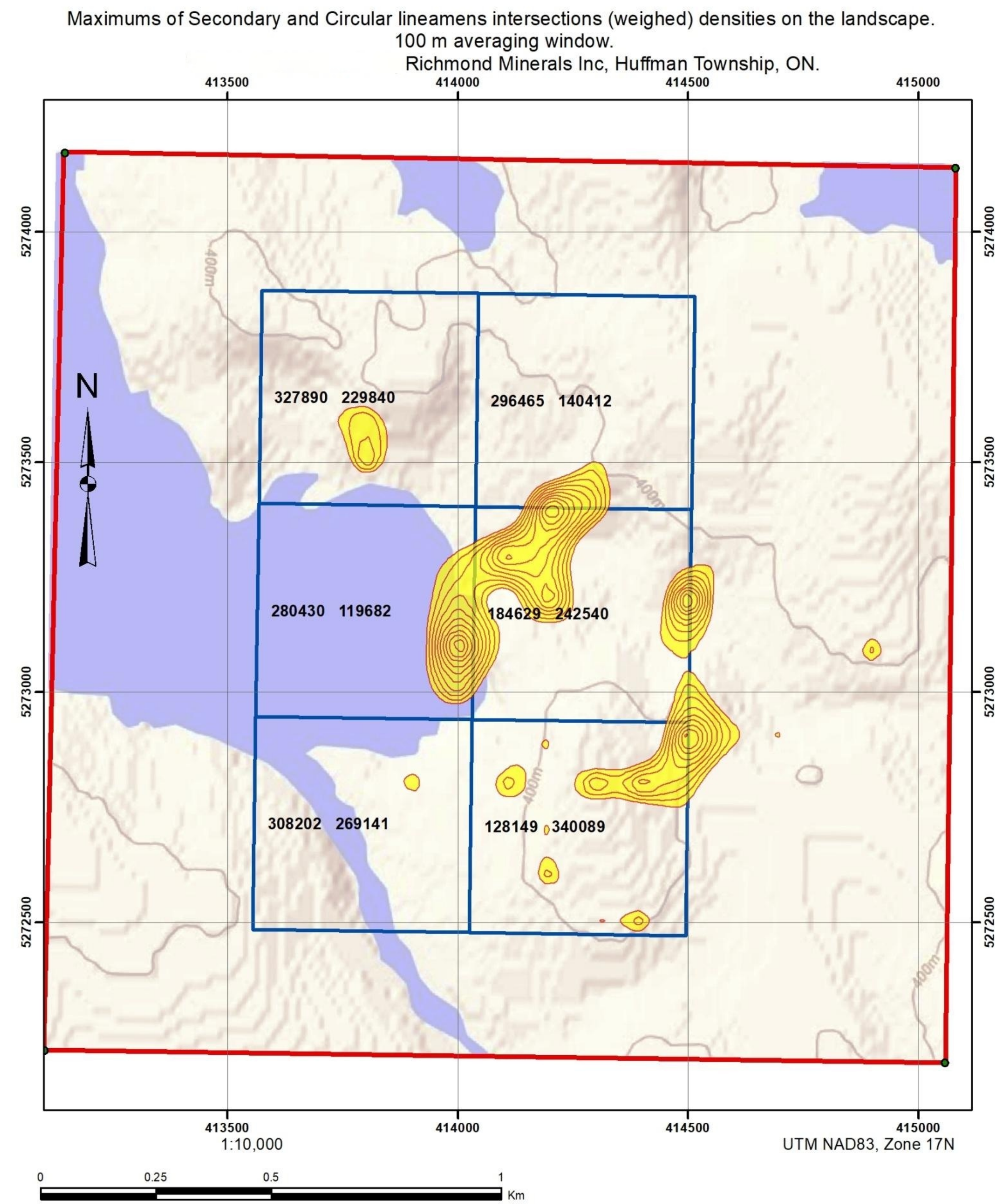

Maximums of Secondary and Circular lineamens intersections (weighed) densities on the landscape.
100 m averaging window.
Richmond Minerals Inc, Huffman Township, ON.
413500
414000
414500
415000
5274000
5273500
5273000
5272500
N
327890 229840
296465 140412
280430 119682
184629 242540
308202 269141
128149 340089
1:10,000
UTM NAD83, Zone 17N
0
0.25
0.5
1
Km

Figure 29.

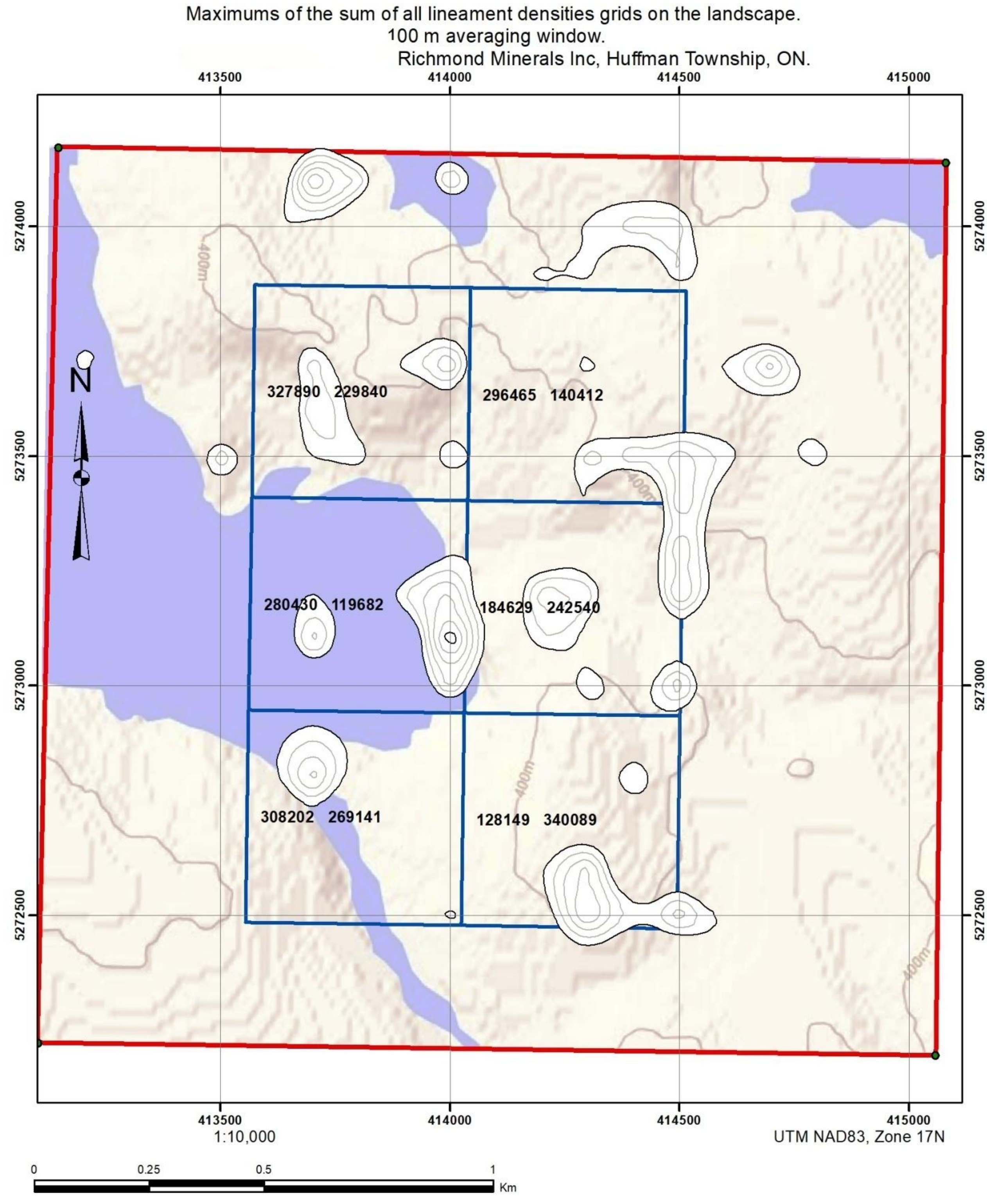
Maximums of the sum of all lineament densities grids on the landscape.
100 m averaging window.
Richmond Minerals Inc, Huffman Township, ON.
413500
414000
414500
415000
5274000
5273500
5273000
5272500
N
327890 229840
296465 140412
280430 119682
184629 242540
308202 269141
128149 340089
400m
1:10,000
UTM NAD83, Zone 17N
0
0.25
0.5
1
Km

Figure 30.

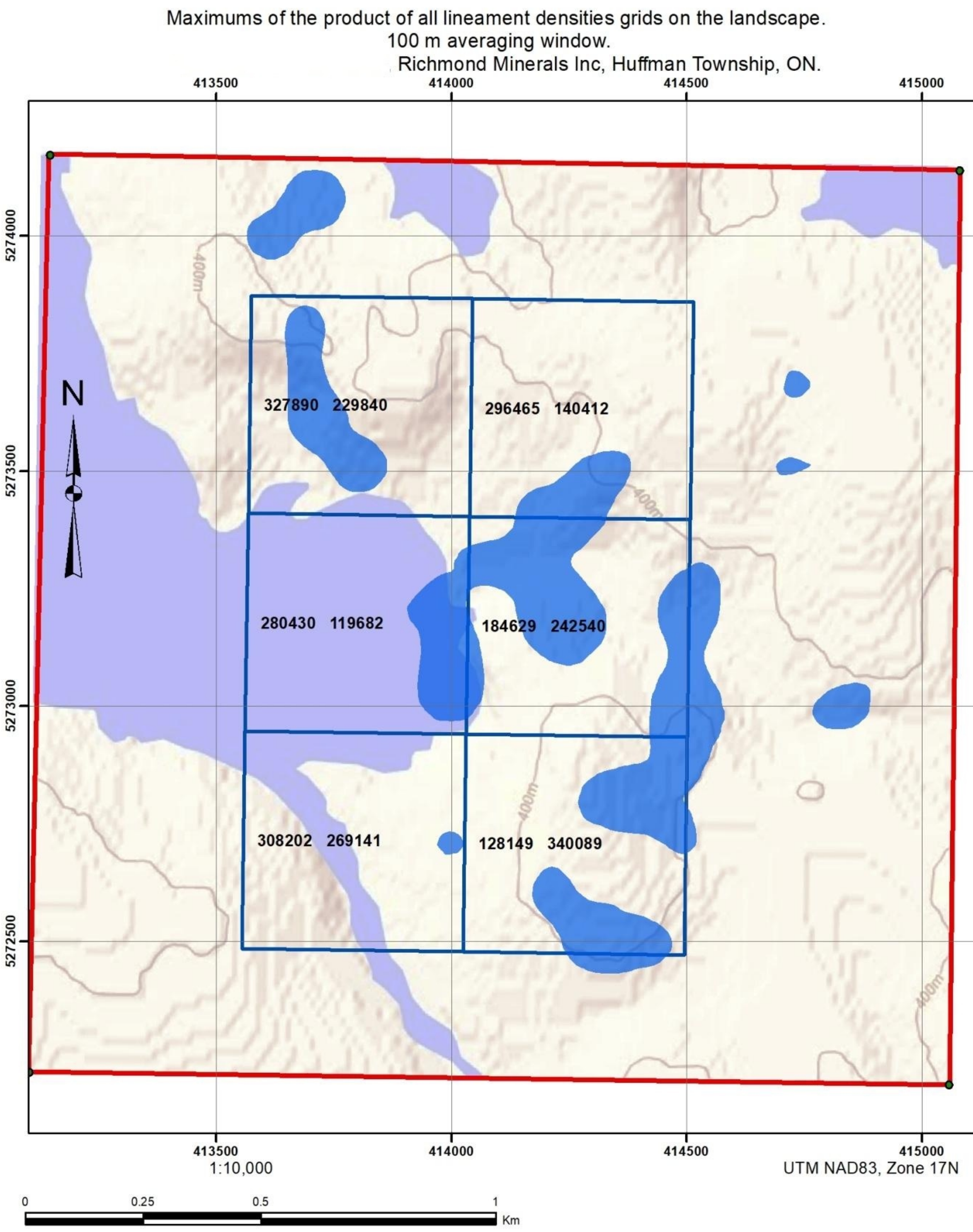
Maximums of the product of all lineament densities grids on the landscape.
100 m averaging window.
Richmond Minerals Inc, Huffman Township, ON.
413500
414000
414500
415000
5274000
5273500
5273000
5272500
N
327890 229840
296465 140412
280430 119682
184629 242540
308202 269141
128149 340089
400m
1:10,000
UTM NAD83, Zone 17N
0
0.25
0.5
1
Km

Figure 31.

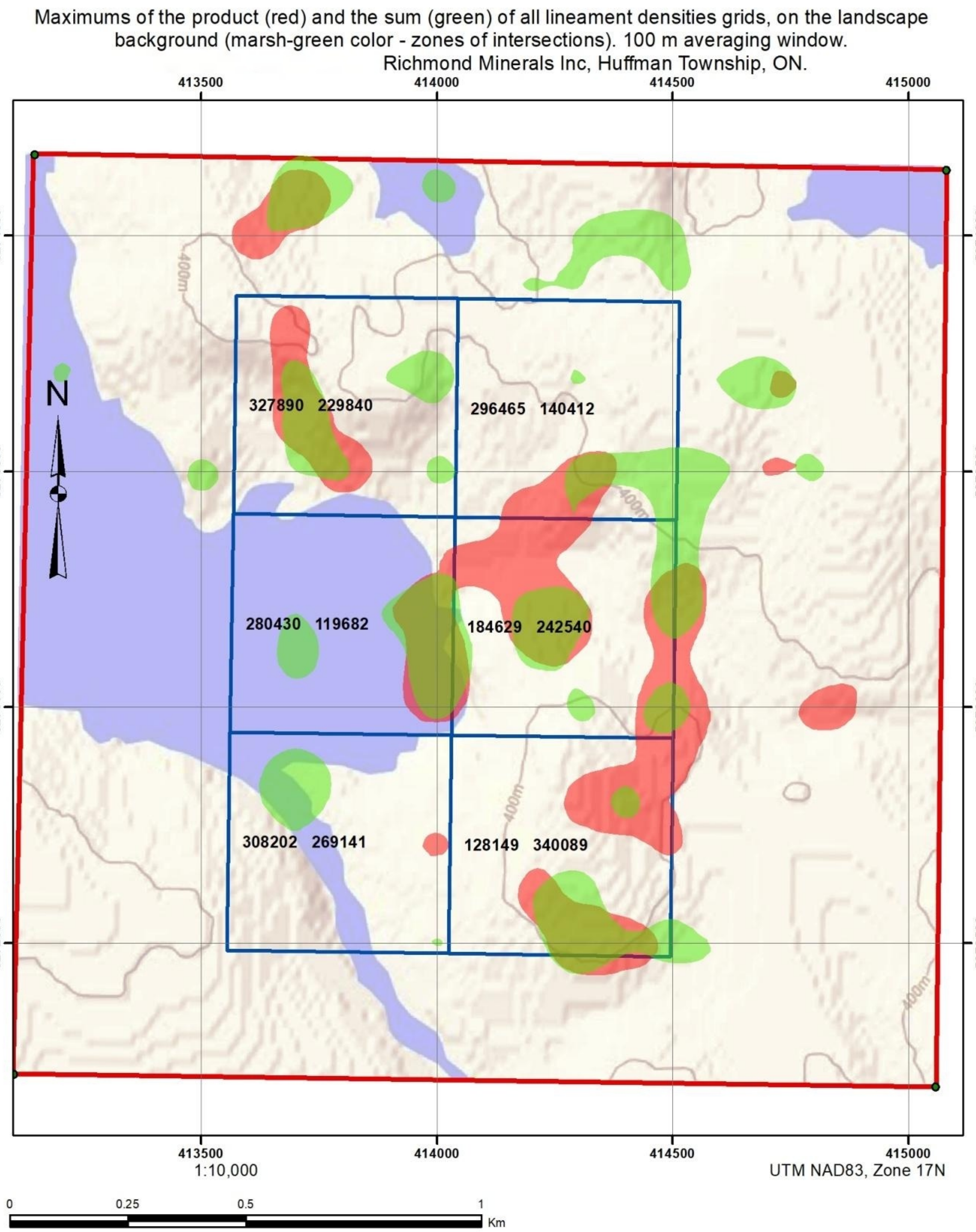
Maximums of the product (red) and the sum (green) of all lineament densities grids, on the landscape background (marsh-green color - zones of intersections). 100 m averaging window.
Richmond Minerals Inc, Huffman Township, ON.
413500
414000
414500
415000
5274000
5273500
5273000
5272500
N
327890 229840
296465 140412
280430 119682
184629 242540
308202 269141
128149 340089
400m
1:10,000
UTM NAD83, Zone 17N
0
0.25
0.5
1
Km

Figure 32.

One question should be discussed with regard to maximum cut-offs. The method is not intended to obey to strict statistical rules. And every region is geologically unique. Same can be said about the lineaments.

Their distribution can be fairy even, and in such case the min-max values of their densities won't be of a huge difference. The cut-offs, say, 60-75% of the max value (or even higher) could be appropriate to map the maximums. As another extreme – the lineament distribution can be very uneven, and cut-offs of 30% of max value can be used. We do not want the maximum to be neither too small-size nor too large. In the first case, one cannot be absolutely sure that there was no error made during the manual procedure of drawing or during the processing. In the second case, one can obtain maximums (targets) which cover more than 50% of the area, and that definitely would not make sense from the exploration standpoint. So, the mapping of the maximums is a compromise between the statistics and practicality. Understanding of this issue becomes particularly important when we walk down the size of the averaging window. The smaller the size the more cautious one will have to be sometimes in terms of choosing the cut-offs.

There is no point in showing all the possible combinations of the contour maps. There are too many of them to put into comprehensive Report. Any combination and consecutive contour maps can be easily produced with common contouring software (Surfer, ArcMap etc.). Tables of lineaments of different averaging windows for such procedure are provided in Digital Delivery Package accompanying the current Report.

From the Remote Exploration Method point of view ANY of these maps (Figures 23-31) may be taken as individual Exploration Target Maps of the first approximation, provided that we know the actual geological correlations between the mineralisation, favorable orientation and the size of some lineaments.

One can see that the maximums may "appear " and "disappear", they become stronger or weaker, they may also shift a bit in the different maps. In most cases we leave on the map in transparent mode. Such presentation allows using a real world image as a background, and helps to avoid irrelevant information.

Now, when we have a set of different maximums combinations, we can overlay these maps onto each other – Figure 33.

****Note, though, that Figures 30 and 31 show the results of somewhat similar to overlaying processes implemented in Surfer mathematically. In Figure 30 we show the maximums of the density grid obtained by summing the grids in Figures 23-29, and in the Figure 31 – the product of those grids. These two maps, and especially their intersection (Figure 32) , are close to the targets, obtained by the processing of the overlay of all the partial (individual) maximum maps of the lineaments and their intersections. It will become clear a bit later in discussion.*

In our view, the averaging window of 100 m size gives the most reliable results – the number of the calculated lineaments is big enough to produce reasonable value, and at the same time is not too big to miss the possible variations in the lineament densities.
There are different ways to build the Target maps based on the partial maximum maps of various lineament densities and maximums of their intersections.

First – manual “old school” approach. We decide, for example, that all the areas where more than a half of the individual maps are overlaid will be considered as the *1st Order Exploration Targets*. If from 4 to 7 maps are overlaid than the area is marked as *2nd Order Target*. Areas with 1-3 layers intersections may be taken as *Areas of Interest*. In case of complex spatial distribution and large number of individual layers this method very often turns to be pretty laborious and time consuming. We did not use this approach in this study. Second approach – formal mathematical procedure which could be divided into 2 main groups:

Multiplication of all grids based on the initial data tables (or multiplication of the table fields). The resulted grid is later processed by applying some suitable (mostly arbitrary) levels of cut-offs. The downside of this approach is that a) the max-min range becomes extremely high in the areas where the calculation windows are not empty (the number of lineaments >0) and b) if any of the grids is empty at certain location then the result (product) at this location is eliminated (multiplication by zero). To avoid the extreme range the normalization of the grids (table fields) can be applied, yet the setting to zero the values in empty cells happens anyway. Surely, the “trick” of assigning the small positive number to empty cells can be used, yet there are no obvious advantages to do so. Another approach would be not to use intersections (since the numbers of intersections are much higher than the numbers of lineaments) but instead stick to the numbers of lineaments only.

Summing the individual grids. This method seems to me the most suitable in most cases, since we deal with the values of the same nature and max-min range still allows seeing simultaneously relatively low values together with the highest ones.

There is no strict rule or advantage with regard to which map building method to apply. Manual technique more easily incorporates into interpretation geological data and other data which are not represented as table datasets or grids. For example, if the favorable conditions for mineralization include some landscape features, particular geological contact, specific fault geometry and so on (data which is difficult to represent as a table dataset), then the manual procedure is more suitable. Yet, it takes much more time than the formal software processing of the table data.

Common sense tells us that the areas on the map where more different and almost independent maps are more perspective for exploration purposes. Such areas demonstrate higher densities of a broad scale range lineaments and their intersections, in this case secondary, main and circular. These areas have a higher permeability for fluid influx, and the dilation pockets are more likely to form within their spatial limits as opposed to other areas.

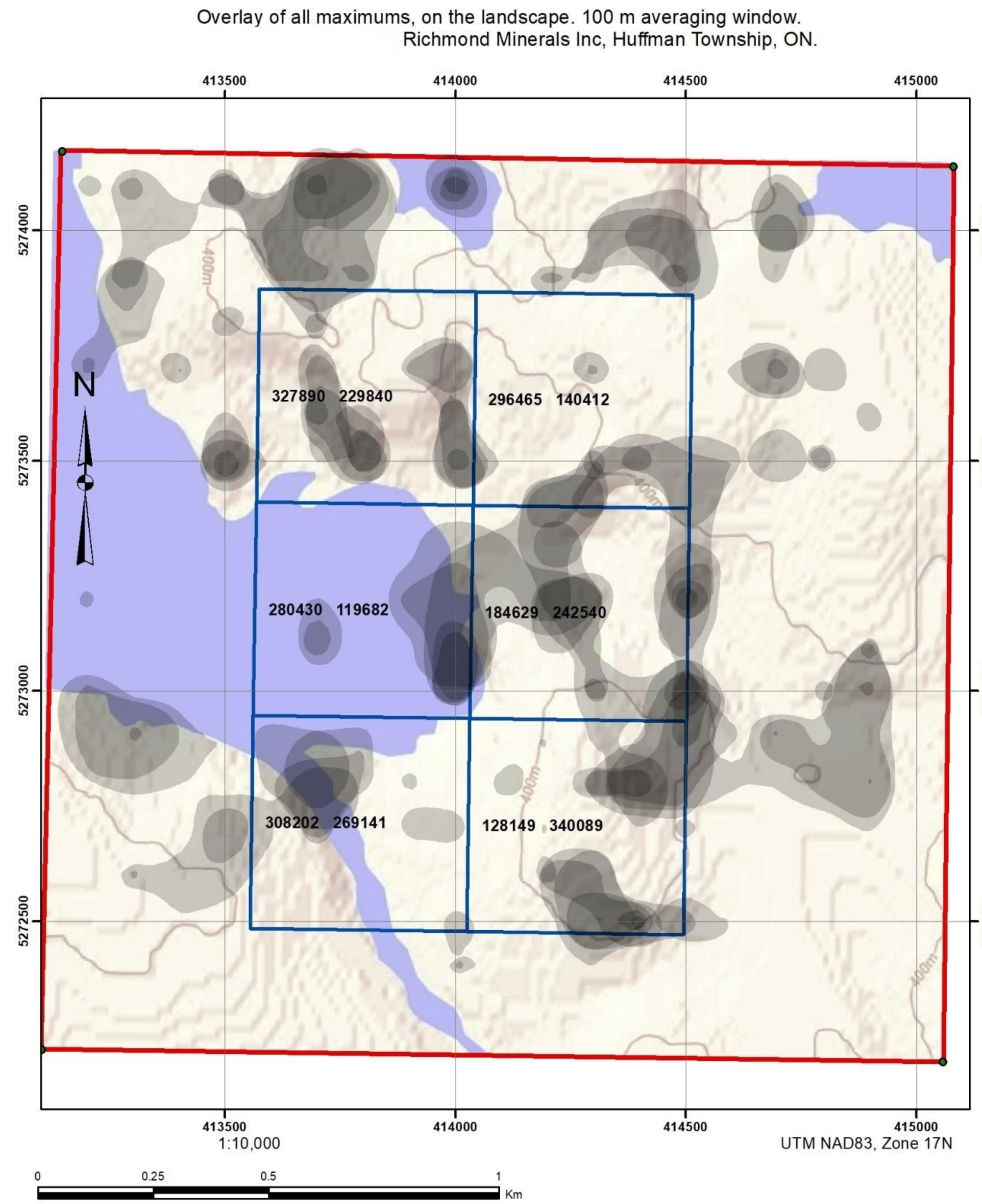

Figure 33.

Therefore, by outlining the areas where most of the different maps intersect we find the 1st Order Exploration Targets. Intersecting areas may be outlined manually, using transparent individual maps; they can be found using special ArcMap tools (*ArcToolBox\Analysis Tools\Overlay\Intersect*); also the grid combination manipulation in Surfer can be used.

We used the Surfer for this particular exercise due to large number of intersection maps. The results are shown in Figure 34.

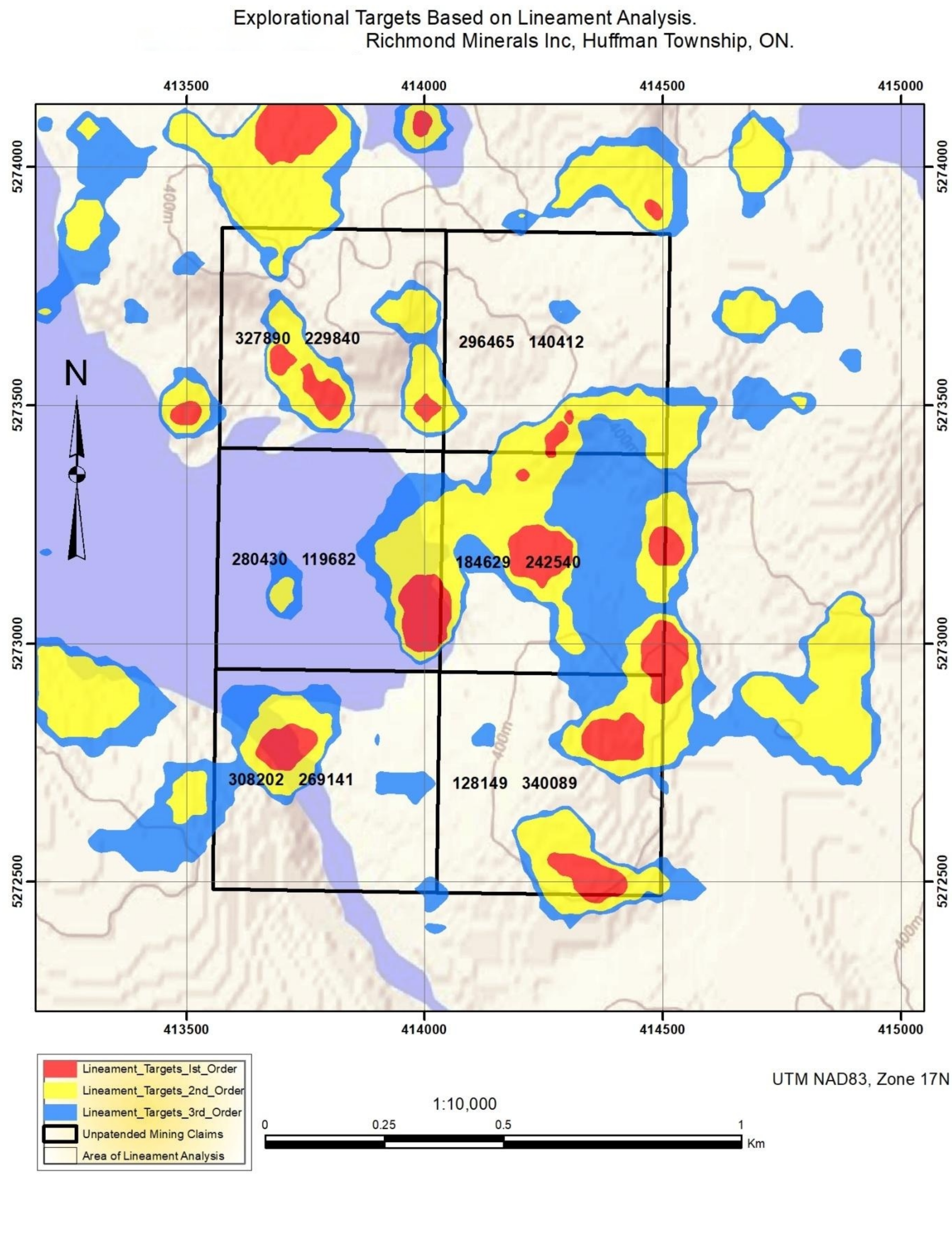

Figure 34.

Zones shown in red are considered as the most favorable for mineralization from the Remote Exploration Method's foundations standpoint and may be recommended as the first target zones for future exploration activities – 1st Order Exploration Targets. Zones in yellow and blue correspond to the Exploration Targets of the 2nd and 3rd Order.

Rose-diagrams - 2-dimensional orientation analysis.

In this study rose diagrams were used to visualize the preferred directions and frequency of the lineaments, and their spatial distribution over the Project Property. Basically, the longer and narrower the peaks in any particular direction is, the stronger and more spatially bound is the lineament system.

Similar to lineament densities calculation, the counting and rose diagram drawings can be made with different averaging window sizes tertiary lineaments.

To process the lineaments and build the diagrams we used the originally designed software.

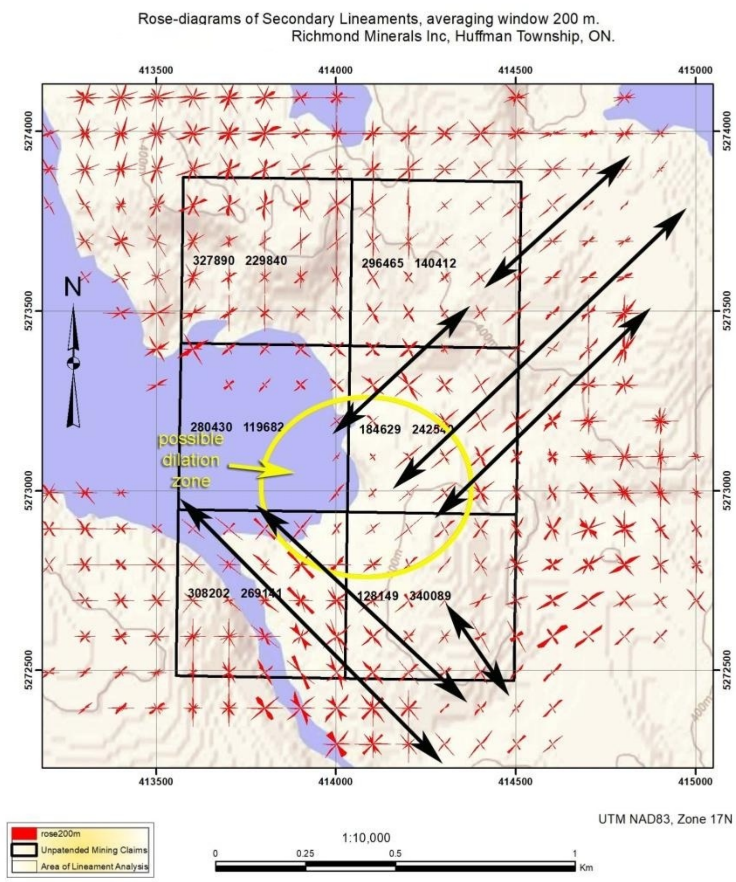

Figure 35. Rose-diagrams of secondary lineaments for the area (200 m averaging window).

For the property scale (Figure 35) two main lineament trends seem to exist (perpendicular to each other) – north-east and north-west. Surely, we do not know the age of the lineaments origin. Yet if we assume that these trends are related to the pre-existing structure before the mineralisation event, then the area where they border may become the zone of dilation during any subsequent deformation. By the same token, it may be the most permeable zone for fluid flow. Therefore, this area may be considered as favorable for mineralization.

Enlargement of the averaging window results in smoothing and even in disappearing of the differences in the lineament orientation trends as it is seen in Figures 36 and 37.

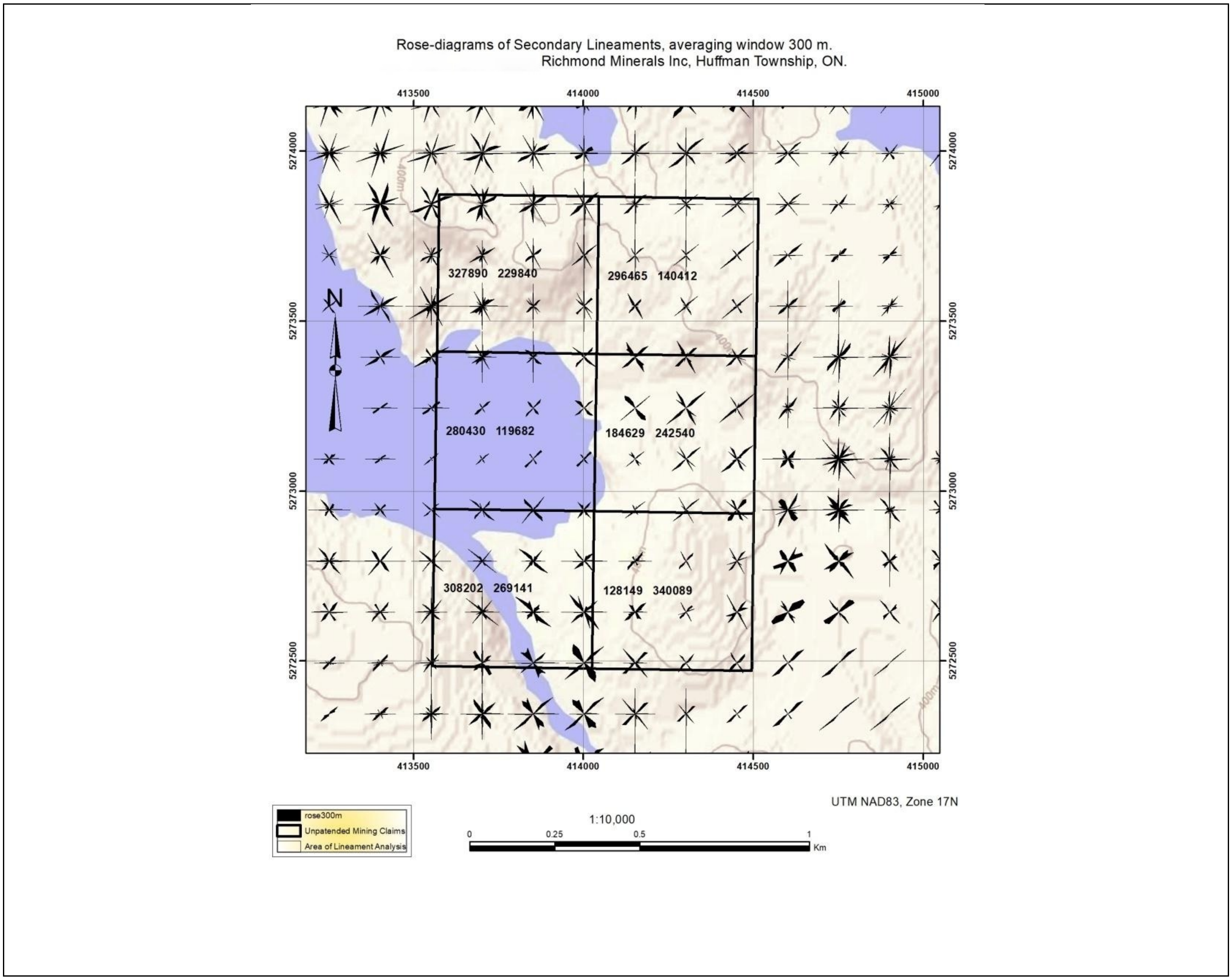

Figure 3613. Rose-diagrams of secondary lineaments for the area (300 m averaging window).

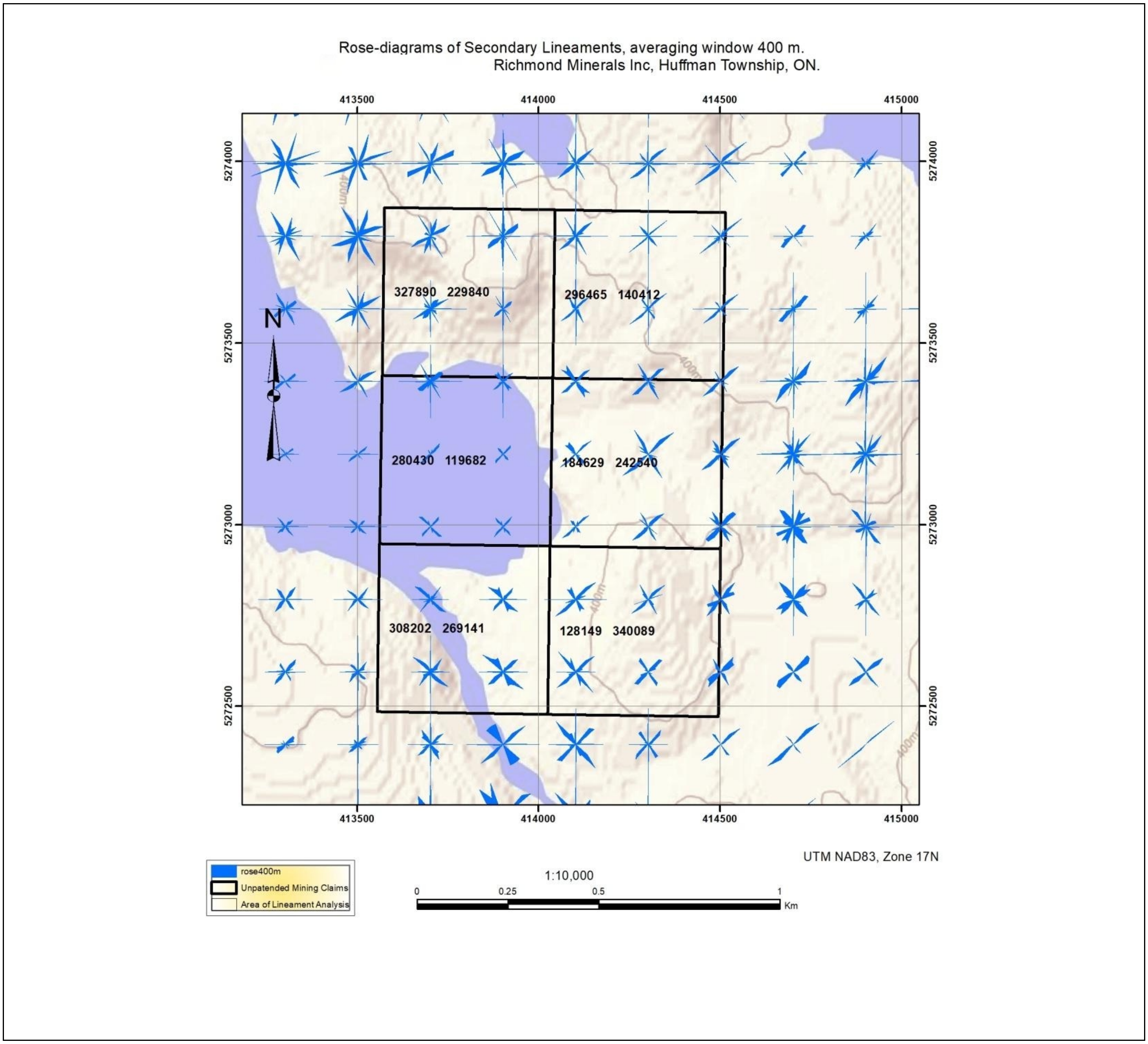

Rose-diagrams of Secondary Lineaments, averaging window 400 m.
Richmond Minerals Inc, Huffman Township, ON.
413500
414000
414500
415000
5274000
5273500
5273000
5272500
N
327890 229840
296465 140412
280430 119682
184629 242540
308202 269141
128149 340089
400m
UTM NAD83, Zone 17N
rose400m
Unpatended Mining Claims
Area of Lineament Analysis
1:10,000
0
0.25
0.5
1
Km

Figure 37.

Physical Modeling.

Plastic deformations modeling.

The fundamentals of the modeling were discussed earlier.

Figure 38 demonstrates the template for the experiments, and it corresponds to the system of the main lineaments.

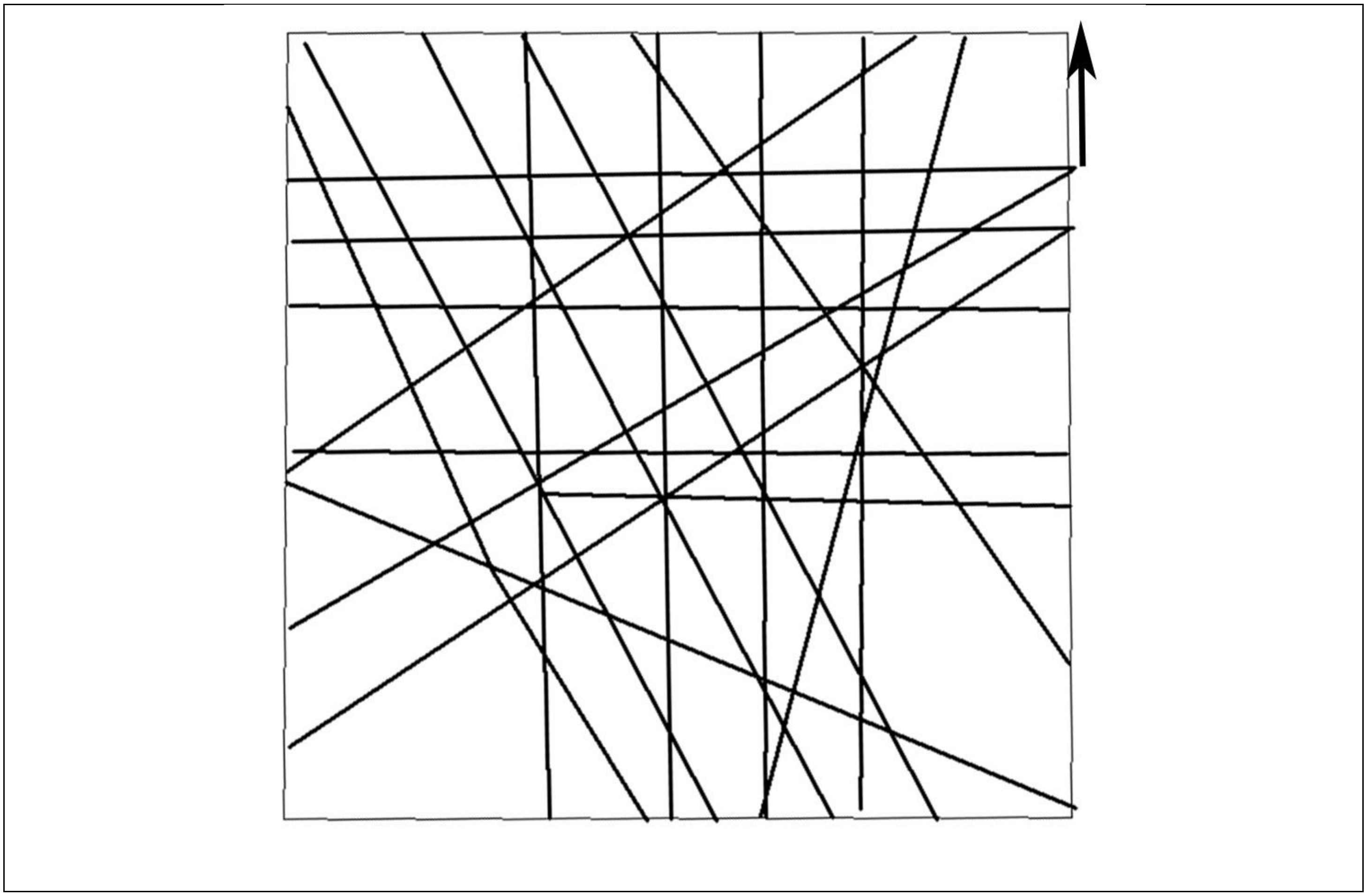

Figure 38. Template for the experiments.

Altogether 12 experiments have been done, out of which we show a few – Figure 39.

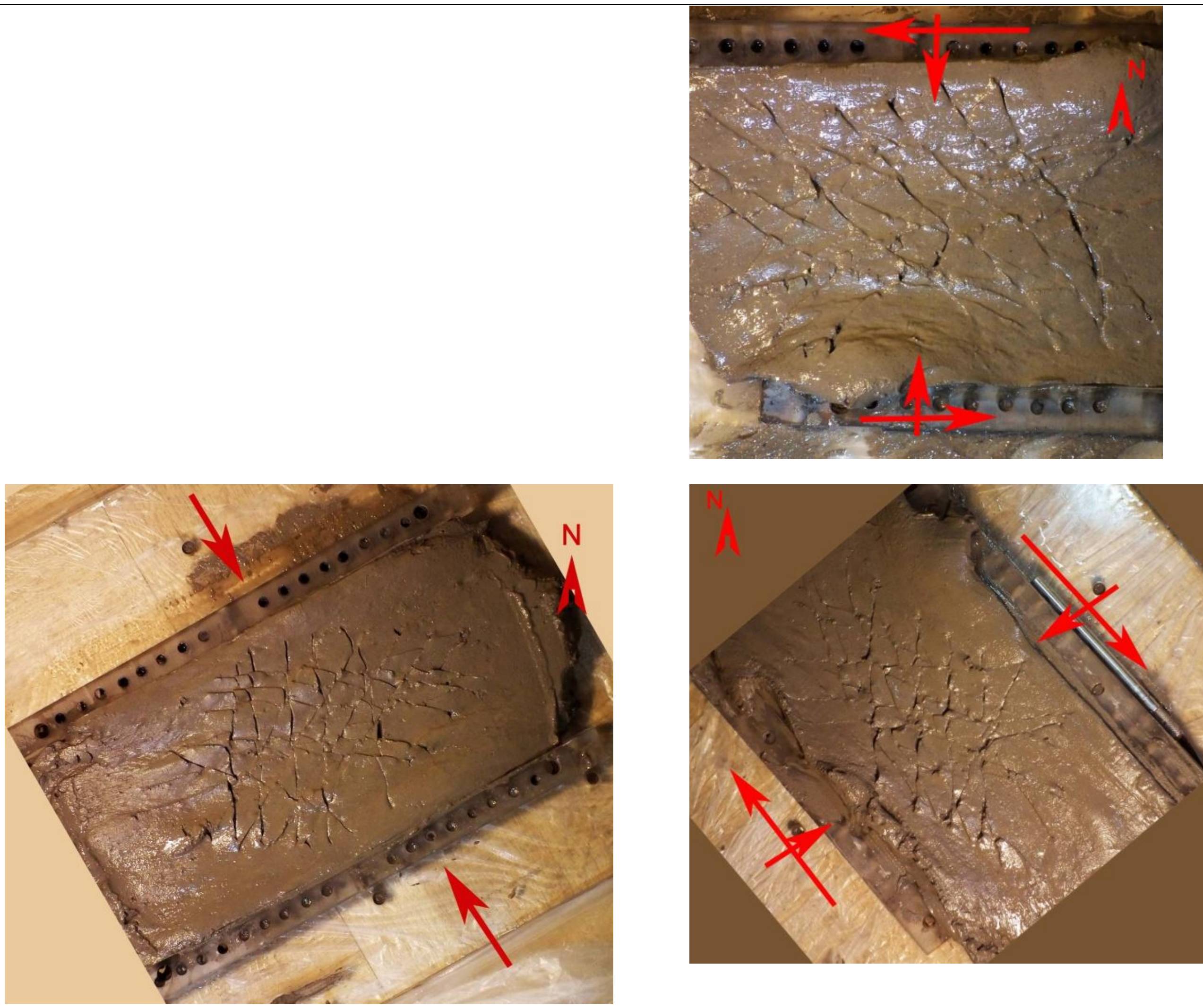

Figure 3914. Some of plastic deformation experiments.

Every experiment was photographed and, then, all the zones of maximal deformations were outlined.

Overlaying all the results onto each other (Figure 40, left) we can find the areas where the deformations always were high (Figure 40, right), and we can also see zones of medium (green), low (blue) and zero (white) deformations.

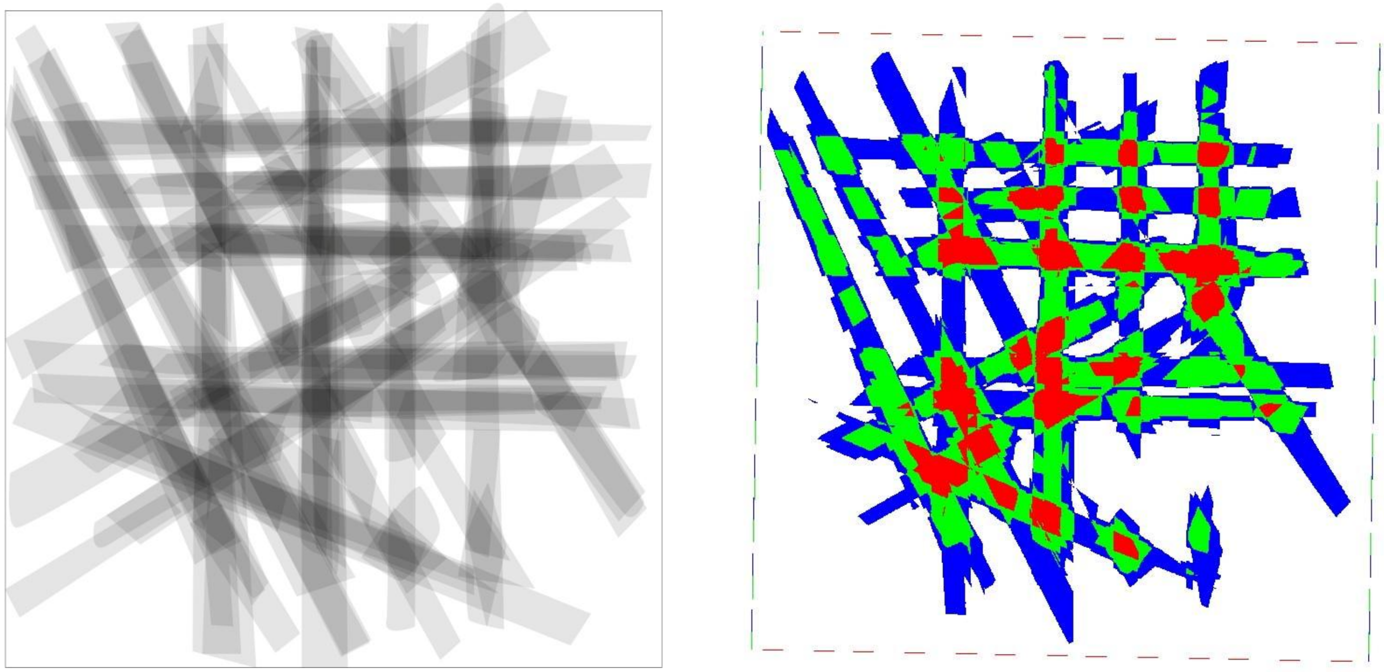

Figure 40. Overlay of all plastic experiments (left) and zones of high (red), medium (green) and low (blue) deformations(right).

Processing the results with specially designed software we also created Surfer contour map for high deformation areas. Plastic group of experiments, basically, suggests that zones of main lineaments intersections represent areas with the highest cumulative deformations. These zones – from the modeling standpoint – may be taken as the most favorable for the future exploration activities – Exploration Targets – Figure 41.

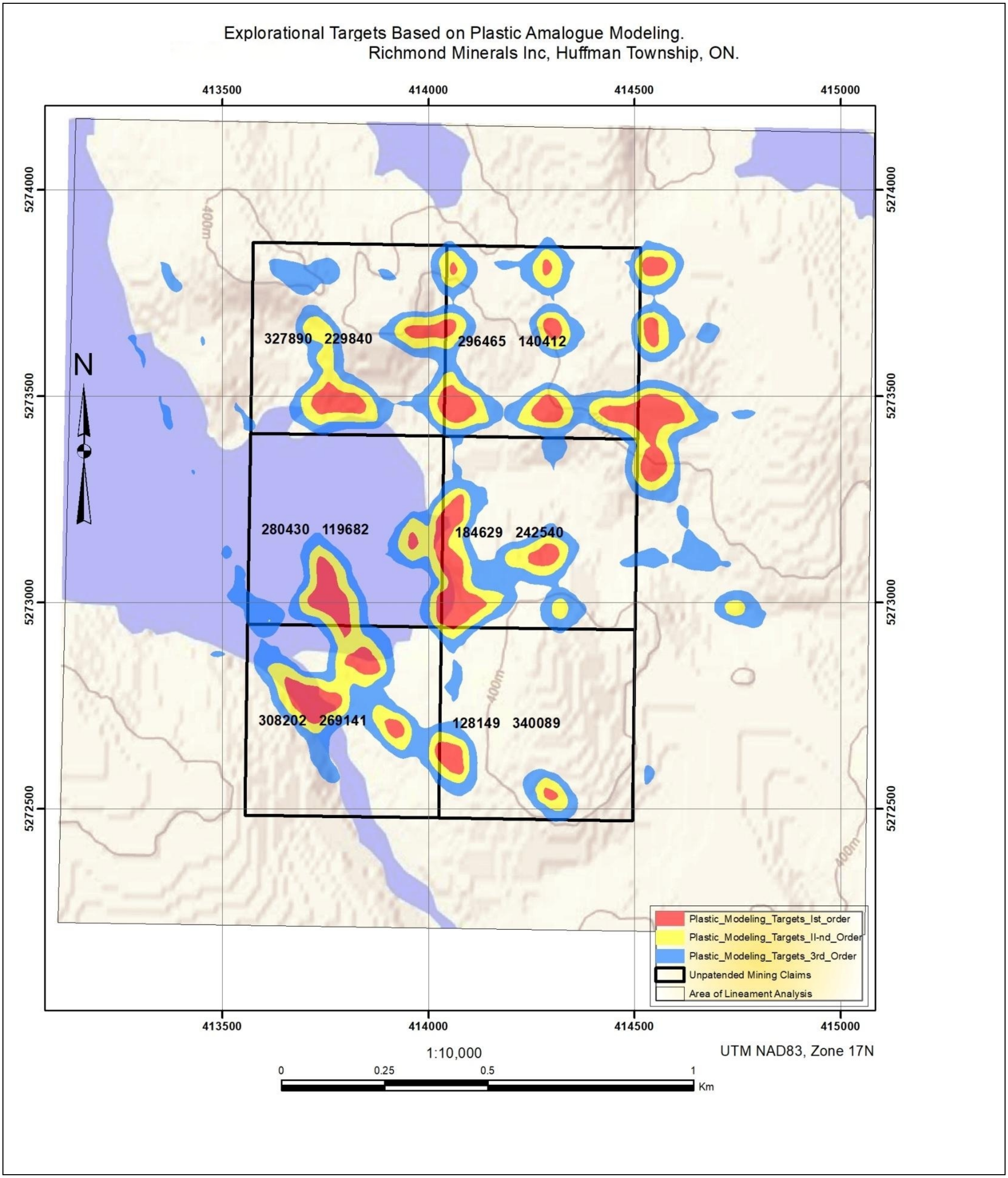
Explorational Targets Based on Plastic Amalogue Modeling.
Richmond Minerals Inc, Huffman Township, ON.
413500
414000
414500
415000
5274000
5273500
5273000
5272500
N
400m
327890 229840
296465 140412
280430 119682
184629 242540
308202 269141
128149 340089
Plastic_Modeling_Targets_Ist_order
Plastic_Modeling_Targets_II-nd_Order
Plastic_Modeling_Targets_3rd_Order
Unpatended Mining Claims
Area of Lineament Analysis
1:10,000
UTM NAD83, Zone 17N
0
0.25
0.5
1
Km

Figure 41.

Elastic Modeling Results.

Altogether 12 experiments have been done; only few are shown – Figure 42.

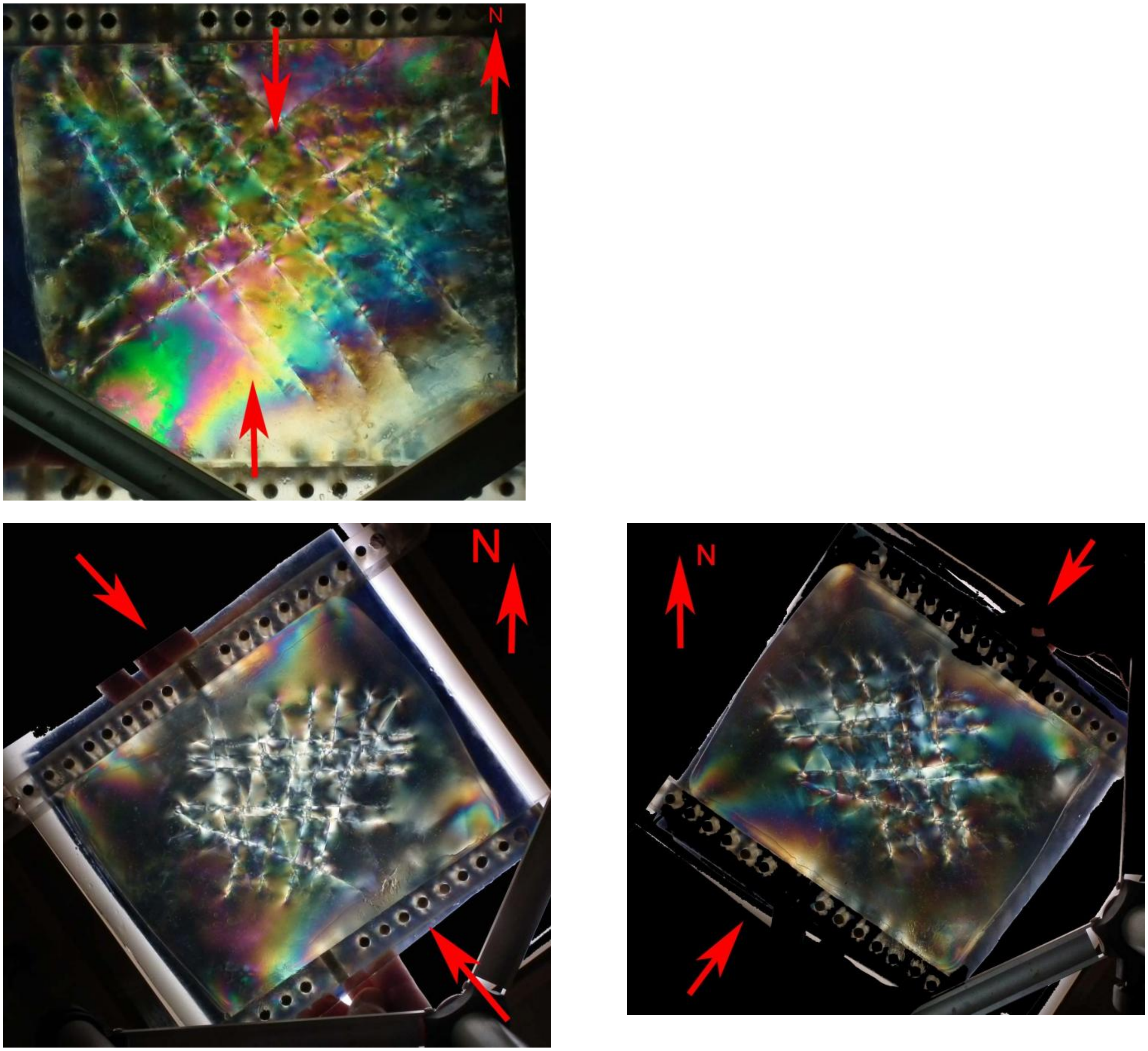

Figure 42. Some of elastic deformation experiments.

Every experiment was photographed and, then, all the zones of maximal deformations were outlined.

For elastic field we are looking for the areas with lowest stresses or dilatational zones. Overlaying all the results onto each other we can find the areas where the deformations always were the lowest (Figure 43).

Elastic group of experiments suggests that most zones of main lineaments intersections represent areas with the lowest stresses. These zones – from the modeling standpoint – may be taken as the most favourable for the future exploration activities Exploration Targets – Figure 55.

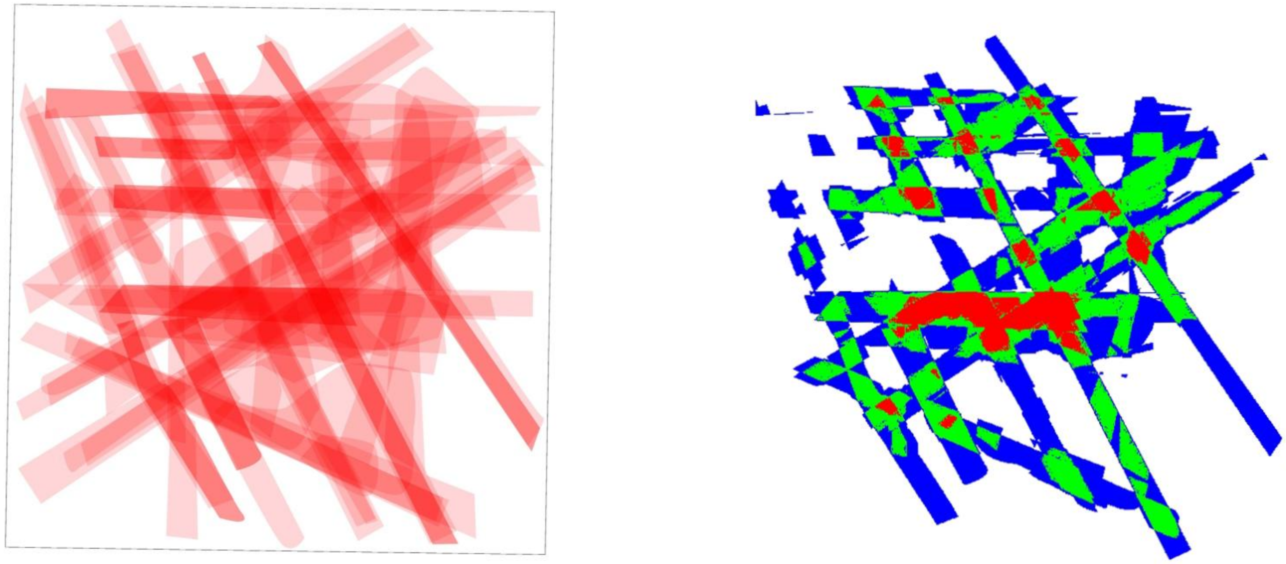

Figure 43. Overlay of all elastic experiments (left) and zones of high (red), medium (green) and low (blue) deformations(right).

This resulted image undergone processing with originally designed software to create a table with the number-values of the deformations in the real coordinate world; the table was, then, converted into Surfer grid and imported into ArcMap. Figure 44 shows the Exploration Targets distribution based on elastic modeling results.

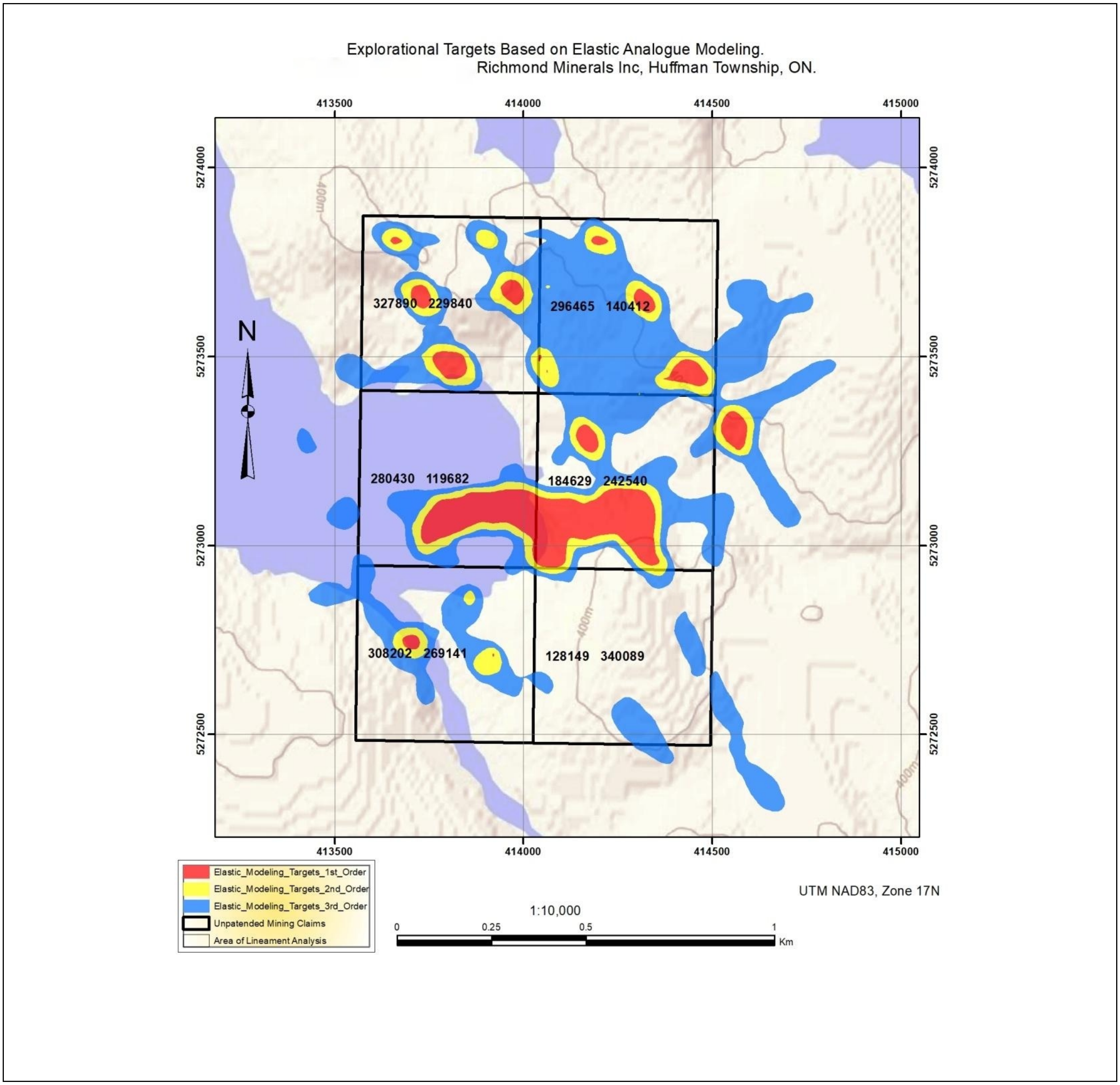

Figure 44.

By overlaying the Targets Maps from Elastic and Plastic Modeling results (Figure 43) we can build the Deformational Exploration Target Map. The Targets are represented by areas where both elastic and plastic modeling targets overlay each other (Figure 45).

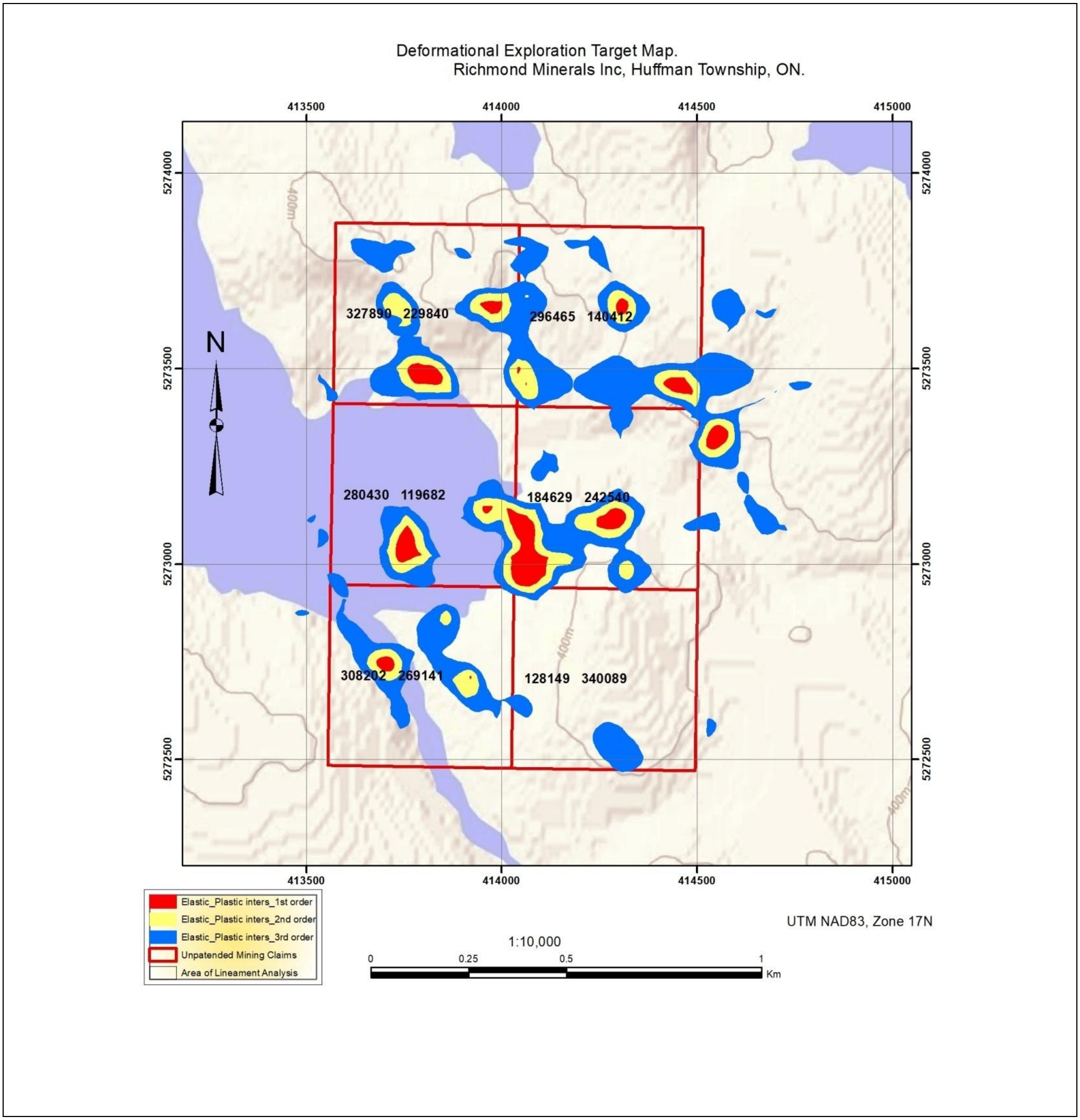
Deformational Exploration Target Map.
Richmond Minerals Inc, Huffman Township, ON.
413500
414000
414500
415000
5274000
5273500
5273000
5272500
N
327890 229840
296465 140412
280430 119682
184629 242540
308202 269141
128149 340089
400m
Elastic_Plastic inters_1st order
Elastic_Plastic inters_2nd order
Elastic_Plastic inters_3rd order
Unpatented Mining Claims
Area of Lineament Analysis
1:10,000
0
0.25
0.5
1
Km
UTM NAD83, Zone 17N

Figure 45.

Combination of Structural Lineament Analysis and Physical Modeling

As we discussed in the corresponding chapters, the density maximums in the lineaments distribution maps most likely represent the areas of maximal permeability of the uppermost earth's crust. This, in turn, should lead to the maximum fluid flow through those zones during geological (and mineralization) history. Same goes to the deformational (strain) maximums of the Plastic Modeling results and to the stress minimums of the Elastic Modeling results. It is these zones that should be taken as *Exploration Targets* in the first place.

Apparently, all the areas where the Lineament Targets and Modeling Targets overlay must be considered as the Primary Exploration Targets.

The Target Maps "reduce" the studied area to just a few most prospective spots and allow planning further exploration with more focus and less money spending.

To build the Primary Exploration Target Maps we need to find the areas of spatial intersection of the Structural Lineament Analysis Targets and Targets obtained from Physical Modeling in Plastic and Elastic fields.

It can be done using ArcMap processing tools.

Figure 46 shows the Primary Target Map obtained by combining the results of Lineament Analysis and Physical Modeling.

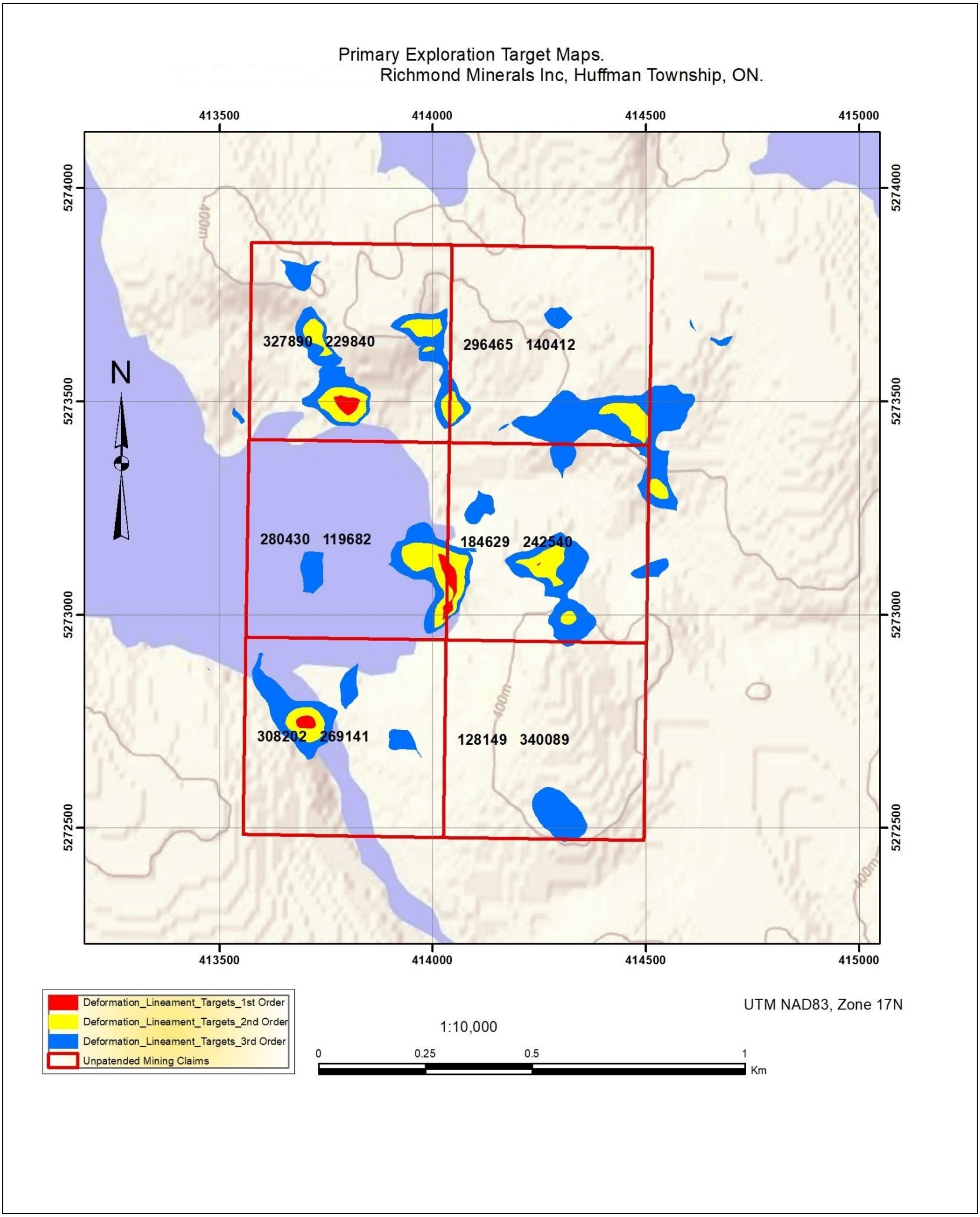

Figure 46. Primary Target Map

Limited sampling results from 2017.

On May 14, 2017, Larry Salo prospected along the shores of Opeepeesway Lake. Using government geology maps he located the contact between the volcanics and the porphyry.

All samples were delivered to ActLabs in Timmins for Gold Fire assay and Silver. Altogether 14 samples have been collected and processed. Unfortunately the silver assays have not returned.

The descriptions of the samples in the report are very sketchy, and the existence of visual molybdenite is not well supported by the included photographs. Yet the gold assays have been done by certified laboratory and should be considered as reliable.

Although there are no very significant gold numbers, few samples ran fraction of gram of gold (Figures 47, 48-50).

Figure 47.

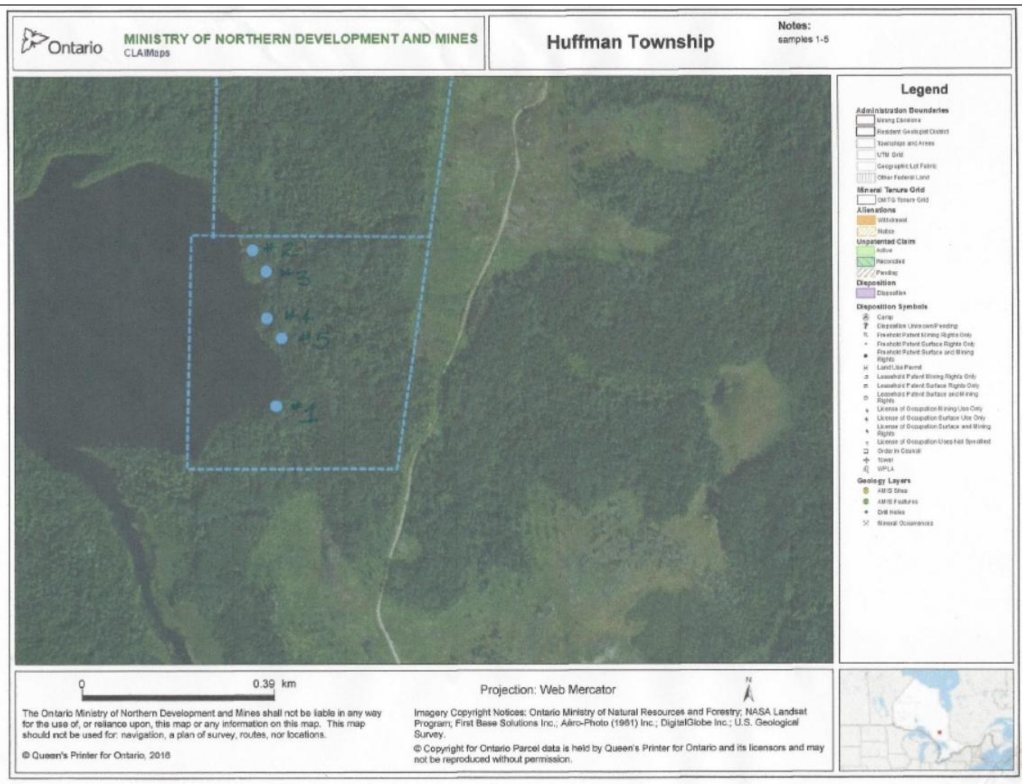

Figure 48. Location of the samples.

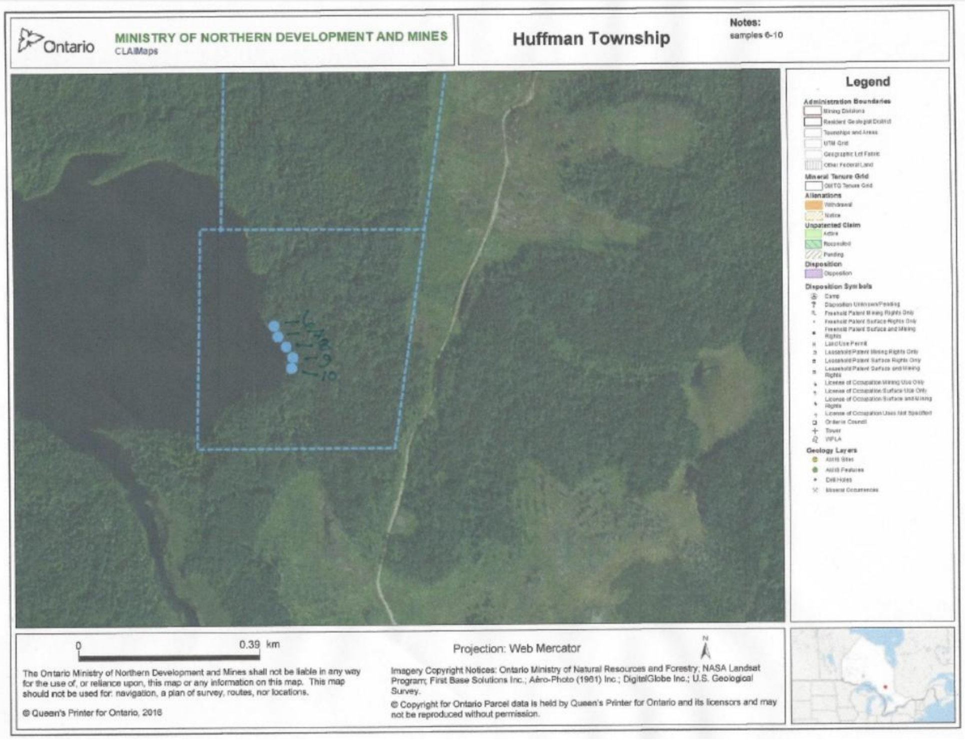

Figure 49. Location of the samples.

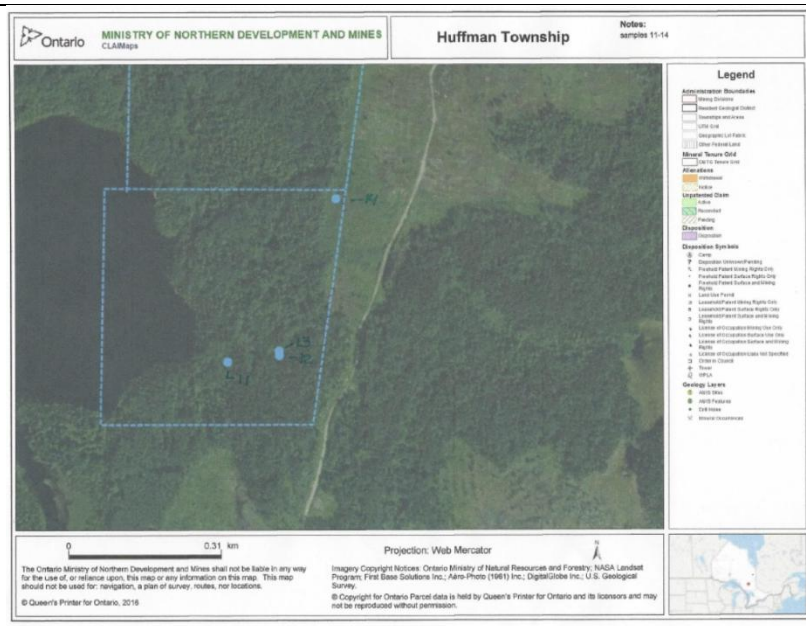

Figure 50. Location of the samples.

Figure 51. demonstrates the gold assays of the grab samples, and Figure 52 – the spatial relationships between anomalous fold values and Primary Targets obtained by the Remote Exploration technique.

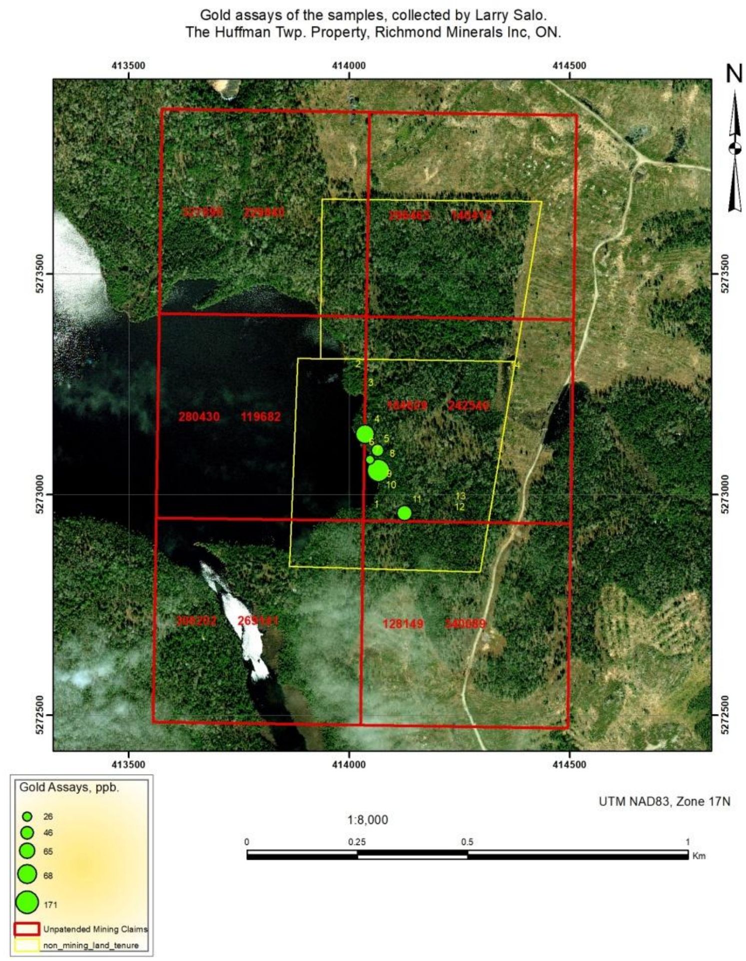
Gold assays of the samples, collected by Larry Salo.
The Huffman Twp. Property, Richmond Minerals Inc, ON.
413500
414000
414500
5273500
5273000
5272500
N
280430
119682
128149
2
3
4
5
6
8
9
10
1
11
13
12
Gold Assays, ppb.
26
46
65
68
171
Unpatended Mining Claims
non_mining_land_tenure
UTM NAD83, Zone 17N
1:8,000
0
0.25
0.5
1
Km

Figure 51.

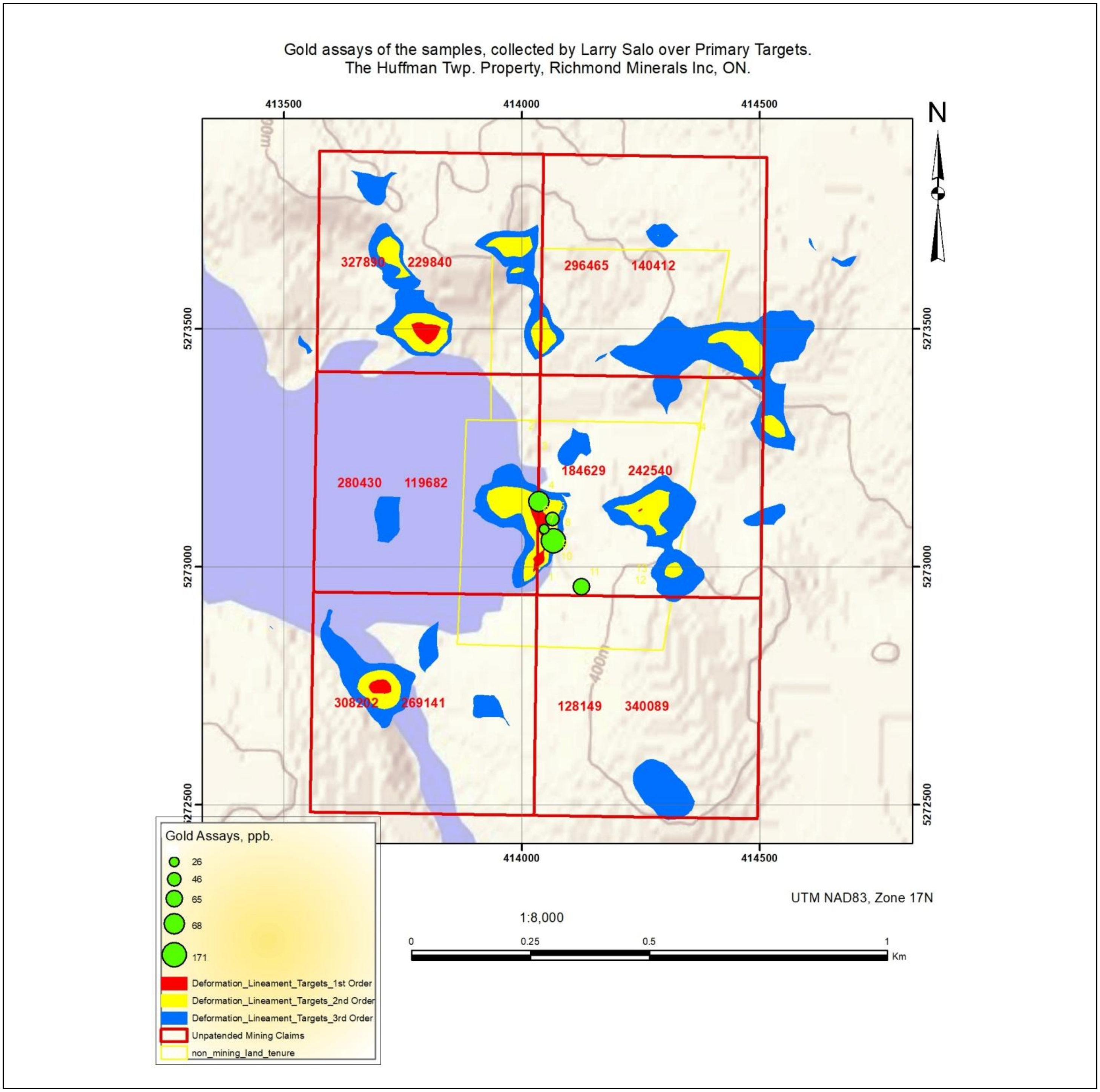

Figure 52.

There is very good correlation between 1st and 2nd Order Targets and anomalous gold content. This area can be considered as one of the first to setup more detail exploration program whether it be ground geophysics, trenching or drilling.

Conclusion

Complex Structural Study of the Huffman Twp. Property (Richmond Minerals Inc) was completed using several different independent datasets. They included optical datasets (satellite images of different resolution and band combinations, aerial photo), topography, and DEM data.

The data were processed into the tables with all the lineaments and their various intersections counts, and additional weighting procedure was applied to the data. All the partial datasets were converted into grids and represented as contour density maximums maps in Surfer and ArcView.

Obtained contour maps of lineament densities repeatedly show areas with high lineament (and their various intersections) densities in several spatially stable locations. These zones are considered as the most favorable for mineralization from the method foundations standpoint, and may be recommended as the first-order target zones for future exploration activities. Although the Exploration Target Maps represent the most reliable targets, the individual Density Maps of lineaments and their intersections may be used for the exploration planning as well.

Rose-diagrams for Secondary lineaments orientation have been constructed. Interpretation of the main lineament trends leads to the assumption that area of the perpendicular orientation trends “collision” may be favorable for fluid flow during the deformation, and consequently, for mineralization.

Analogue modeling (plastic/rupture and elastic fields) results show that there exist some spatially stable zones with the highest deformation and fracturing (plastic) or the lowest stress (elastic) in various geodynamic stress fields. These zones – from the modeling standpoint – may be taken as the most favorable for the future exploration activities. The Exploration Target Maps based on the Modeling have been built.

By combining the results obtained by Structural Lineament Analysis and Physical Modeling we built Primary Target Map. From the Complex Structural Analysis standpoint, these targets should be taken as the areas for the future exploration activities.

It is also important to use the partial (not final) target maps obtained by separate processing stages of Remote Exploration Method.

Further improvements of the target maps can result from the updating the existing maps with field structural observations, geochemical and/or geophysical surveys.

References:

Jonathan Selby, Patterns in the crust: a key to ore discovery, Geology Today, September-October 1987:160-164

Carlos J. Chernicoff, Jeremy P. Richards, Eduardo O. Zappettini. Crustal lineament control on magmatism and mineralization in northwestern Argentina: geological, geophysical, and remote sensing evidence, Ore Geology Reviews, 21 (2002) 127–155

James F. Doyle, James W. Phillips , Daniel Post. Manual on Experimental Stress Analysis (fifth edition). Society for Experimental Mechanics (1989)

J. SALO – Sampling Results, June 12 2017. 2254022 ONTARIO LTD.